ENGINEERING RESEARCH INSTITUTE
UNIVERSITY OF MICHIGAN
ANN ARBOR

STRESS-STRAIN RELATIONS IN PLASTICITY AND RELATED TOPICS

TECHNICAL REPORT NO. 2

AN EXPERIMENTAL STUDY OF BIAXIAL STRESS-STRAIN RELATIONS IN PLASTICITY

By

P. M. NAGHDI

J. C. ROWLEY

Project 2027

OFFICE OF ORDNANCE RESEARCH, U.S. ARMY
CONTRACT DA-20-018-ORD-12099
PROJECT NO. TB 20001(234), DA PROJECT 599-01-004

December, 1953

ACKNOWLEDGMENTS

The authors wish to express their appreciation to Messers. C. W. Beadle and G. A. Shifrin, Research Assistants in Engineering Mechanics, for their valuable assistance, both in the improvement of the extensometer and other equipment and in the running of tests.

ABSTRACT

Experimental results for 10 tubular 24 S-T4 aluminum-alloy specimens are reported. The data from these variable-loading path tests under the action of combined tension and torsion are presented and discussed. Included in an appendix is a description of modifications of the experimental equipment given previously.

AN EXPERIMENTAL STUDY OF BIAXIAL STRESS-STRAIN RELATIONS IN PLASTICITY

1. Introduction

Although considerable progress has been made in recent years in the development of initially isotropic theories of plasticity for strain-hardening materials[1,2], relatively little is known about initially anisotropic theories of plasticity which account for such phenomenon as the Bauschinger effect[3]. This is not surprising, since at present too few experimental results are available. To correlate test results with initially isotropic theories of plasticity, some experimenters in the past have made considerable efforts to use test specimens which are reasonably isotropic and uniform. In almost all cases reported, however, it seems to have been difficult to eliminate the nonuniformity and initial anisotropy of the material. Hence, correlation of experimental results with initially isotropic theories of plasticity is only qualitative in nature. Such correlation may, of course, lay the groundwork for further progress in the development of more general theories to account for initial anisotropy, as well as such phenomena as the Bauschinger effect.

The present report contains experimental results for 10 tubular specimens subjected to the combined action of tension and torsion with variable loading paths. The tubular specimens, which were made of 24S-T4 aluminum alloy, possessed considerable initial anisotropy*. Also discussed is the significance of the experimental results in the light of the general theory of plasticity.

2. General Background

For initially isotropic and plastically incompressible strain-hardening materials, two distinct theories of plasticity (flow and deformation) have been employed in recent years. The basic concepts and

*See Reference 4.

consequences of these theories have been discussed by Prager[1,2]; while illuminating discussions of the role of the experiments, as well as their correlation with the mathematical theory of plasticity in general, and interpretation of experimental results have been given by Drucker[5,6,7] and Prager[8]. Both of these theories are linear in character; i.e., the linearity of increments of plastic strains in the increments of stress is assumed. It may be mentioned that the slip theory of plasticity[9], which has been regarded as a nonlinear theory, has recently been shown by Koiter[10] to be included in the class of linear flow theories which are associated with singular yield conditions.

While stress-strain relations of the deformation type are valid for radial loading paths (i.e., loading for which all components of stress increase at the same rate), they are invalid for more complex paths of loading. For such paths, stress-strain relations of the flow type must be used.

For purposes of clarity, we shall discuss briefly the general stress-strain relations of flow and deformation theories and their consequences relevant to the experimental results given in this report.

The general flow theory which incorporates the history of loading, when expressed in terms of plastic potential f, reads as follows:

$$\dot{\epsilon}''_{ij} = H \frac{\partial f}{\partial \sigma_{ij}} \frac{\partial f}{\partial \sigma_{k\ell}} \dot{\sigma}_{k\ell} \quad \text{for loading, i.e.,} \quad \frac{\partial f}{\partial \sigma_{k\ell}} \dot{\sigma}_{k\ell} > 0$$

$$= 0 \quad \text{for unloading or neutral loading, i.e.,} \quad \frac{\partial f}{\partial \sigma_{k\ell}} \dot{\sigma}_{k\ell} \leq 0 \ . \qquad (1)$$

H is a scalar function which may depend on state of stress (σ_{ij}), strain (ϵ_{ij}), and/or history of loading. In (1), the dot denotes differentiation with respect to time, and prime and double primes refer to the elastic and plastic components of strain, as it is tacitly assumed that the total strain tensor $\epsilon_{ij} = \epsilon'_{ij} + \epsilon''_{ij}$.

The loading function (yield condition) f in (1) may be such as to account for various degrees of initial and strain-hardening anisotropy. A few loading functions exhibiting this character have been suggested by Edleman and Drucker[3]. A simple example is

$$f = \frac{1}{2} C_{ijk\ell} \, \sigma_{ij} \, \sigma_{k\ell} \ , \qquad (2)$$

which accounts for small initial anisotropy. In (2), $C_{ijk\ell}$ is a symmetric tensor of quadratic form.

For isotropic theories of plasticity, f may be a function of both σ_{ij} and ϵ_{ij}. When f is a function of σ_{ij} alone, then the flow theory is referred to as the isotropic stress theory. In this connection, it is clear that the simple flow theory

$$\dot{\epsilon}''_{ij} = H(J_2)\, S_{ij}\, \dot{J}_2 \tag{3}$$

may be obtained directly from (1), if H is assumed to depend on only J_2, and when $f = J_2$, i.e.,

$$J_2 = \frac{1}{2} S_{ij} S_{ij} . \tag{4}$$

In (3), the stress deviation S_{ij} is given by

$$S_{ij} = \sigma_{ij} - S\,\delta_{ij} \; ; \quad S = \frac{1}{3}\sigma_{ii} , \tag{5}$$

where δ_{ij} is the Kronecker delta.

The stress-strain relations of the deformation type for initially isotropic strain-hardening materials have been given with complete generality by Prager[11]:

$$\epsilon''_{ij} = \underline{P}(J_2, J_3)\, S_{ij} + Q(J_2, J_3)\, t_{ij} , \tag{6}$$

where J_2 is given by (4) and

$$\left.\begin{aligned} J_3 &= \frac{1}{3} S_{ij} S_{jk} S_{ki} \\ t_{ij} &= S_{ik} S_{kj} - \frac{2}{3} J_2\, \delta_{ij} . \end{aligned}\right\} \tag{7}$$

It is easily seen that the simple deformation theory

$$\epsilon''_{ij} = \underline{P}(J_2)\, S_{ij} \tag{8}$$

is a special case of equation (6).

In the experiments on tubular specimens which are to be described, the loading was such that tension alone was followed by torsion (accompanied by various amounts of tension); and the determination of the initial shear modulus G_i when twist began was included. For this reason, it is desirable to examine the predictions of various theories of plasticity appropriate for such loading paths, with reference to the initial shear modulus G_i.

As has been pointed out previously*, all isotropic deformation theories predict that the initial shear modulus is given by

$$G_i = \frac{G_o}{1 + 3G_o\left(\frac{1}{E_s} - \frac{1}{E_o}\right)} \quad \text{for loading}$$

$$= G_o \quad \text{for unloading,} \tag{9}$$

where E_s is the secant modulus with reference to the initiation of twist, and E_o and G_o are the elastic moduli in tension and shear.

Similarly, all linear isotropic flow theories of plasticity imply that (for all $d\sigma_{33}/d\sigma_{23} = d\sigma/d\tau$)

$$G_i = G_o \quad \text{for both loading and unloading.} \tag{10}$$

If, however, in equation (1) f is an anisotropic loading function, then during loading G_i will not necessarily be equal to G_o. In particular, if f is assumed to be of the form given by (2), then

$$G_i = \left.\frac{d\sigma_{23}}{2\,[d\epsilon''_{23} + d\epsilon'_{23}]}\right|_{\sigma_{23}=0} = \frac{G_o}{1 + G_o\, H\, \sigma^2\, (C_{1211})\, [C_{1111}\frac{d\sigma}{d\tau} + 2C_{1211}]}\,.$$

*See, for instance, Reference 12.

3. Experimental Results

The experiments performed on 10 thin-walled tubular specimens will be described, and their results will be presented in this section. These variable-loading-path tests consist of tension alone, followed by torsion and varying amounts of accompanying tension. The test specimens and their data have been arranged in four groups (designated as A, B, C, D) according to the value of the ratio of tension to torsion at the initiation of the torque. This grouping is indicated in Fig. 1, where, in conformity with engineering notation, σ_z and $\tau_{\theta z}$ (or simply σ and τ) denote the axial and shearing stresses in the tubular specimen. Also shown in Fig. 1 is the approximate value of the initial slope $d\sigma/d\tau$ for each group.

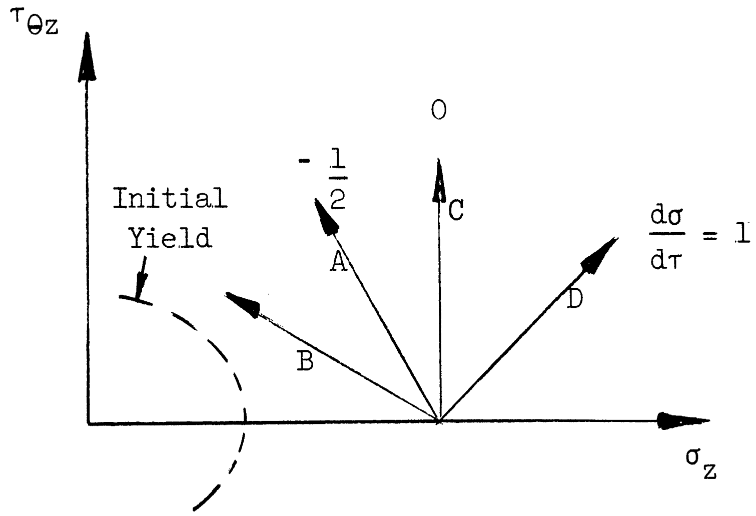

Fig. 1

The test data obtained are presented in the form of curves, in Figs. 2 - 11. For each group of specimens, three sets of curves are plotted: axial stress vs. axial strain, showing where twist began; elastic and initial shear moduli, including two elastic runs before and after each experiment (the first run was performed on the virgin tube in each case); and plastic strains occurring after initiation of twist. In each group, the secant modulus was computed to be approximately 7 x 10^6 psi.

In the data computations, the following formulas were used:

Axial strain $\epsilon_z = \frac{\ell - \ell_0}{\ell_0}$,

where ℓ_0 is the initial gage length.

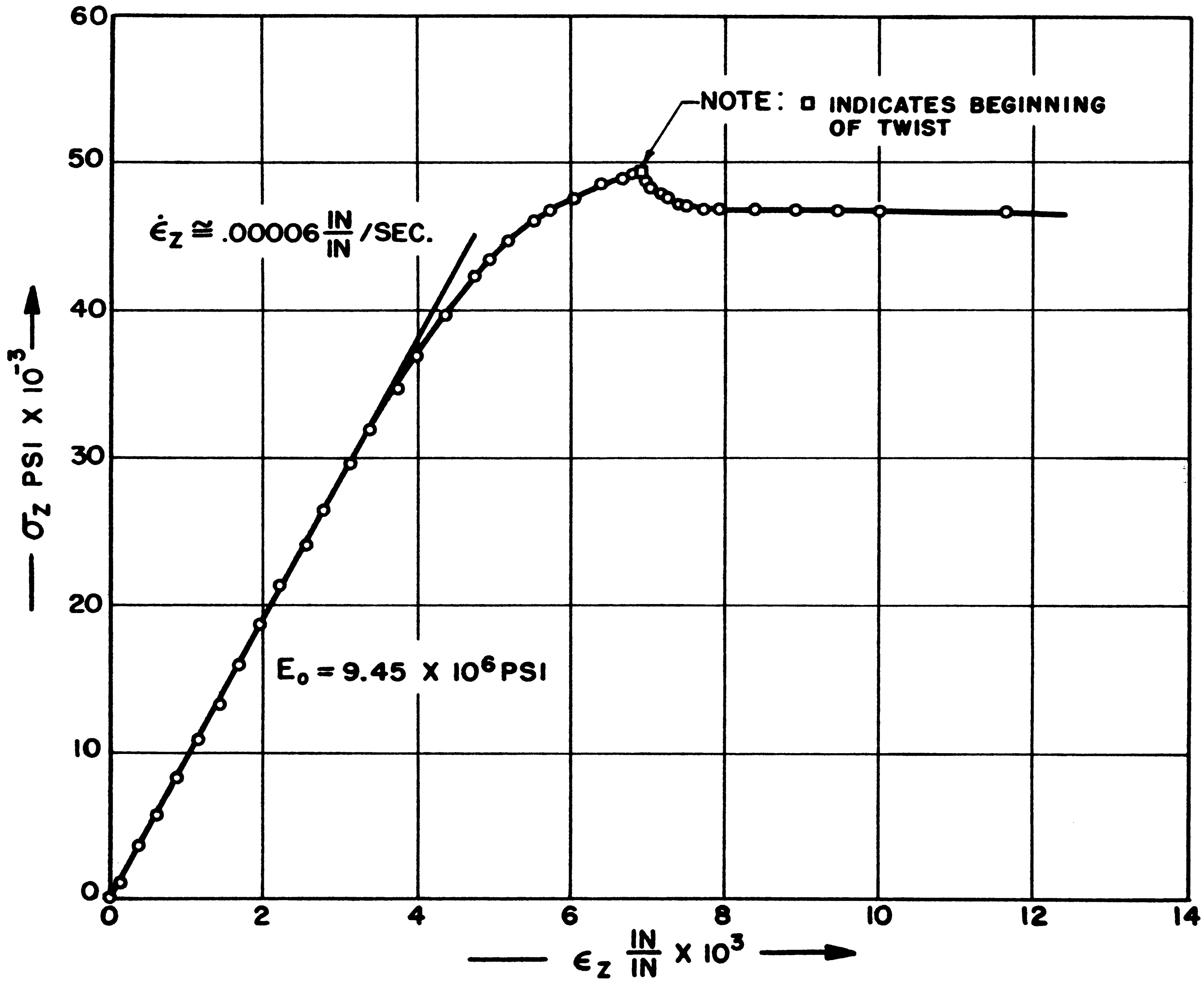

FIG. 2(a) AXIAL STRESS vs. AXIAL STRAIN
TUBE A-1 (#27)

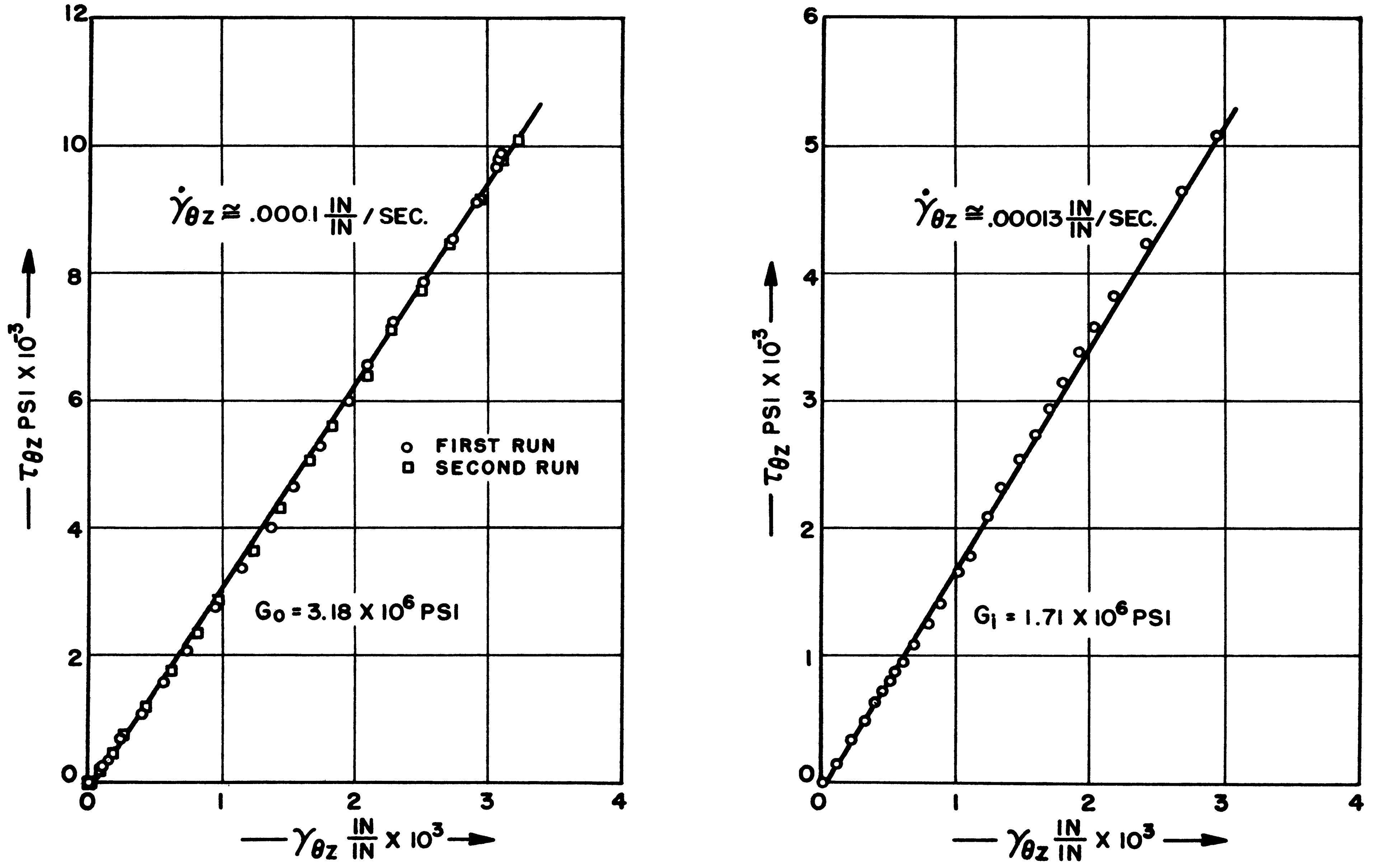

FIG. 2(b) ELASTIC AND INITIAL SHEAR MODULI
TUBE A-1 (#27)

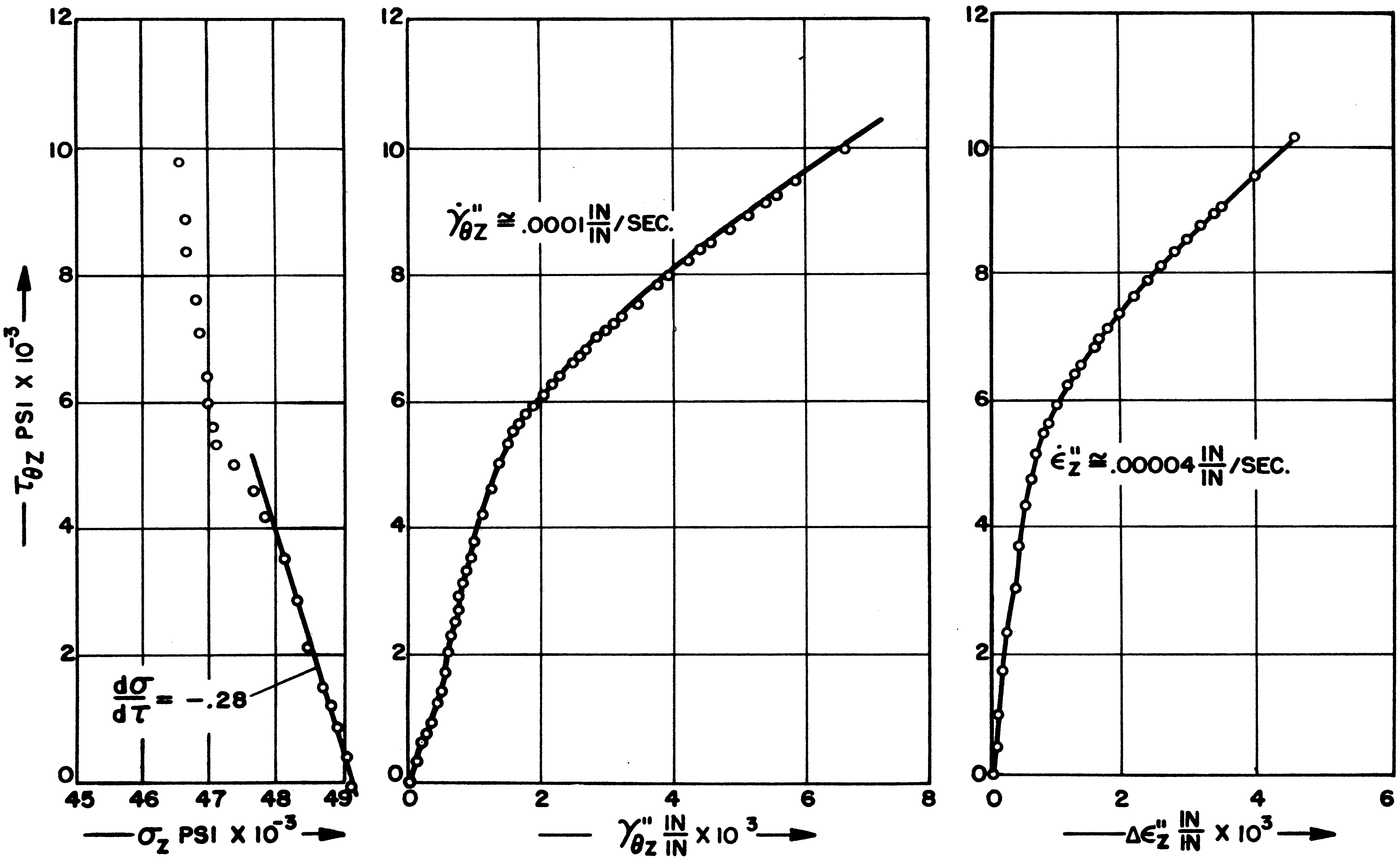

FIG. 2(c) PLASTIC STRAINS AND LOADING PATH
TUBE A-1 (#27)

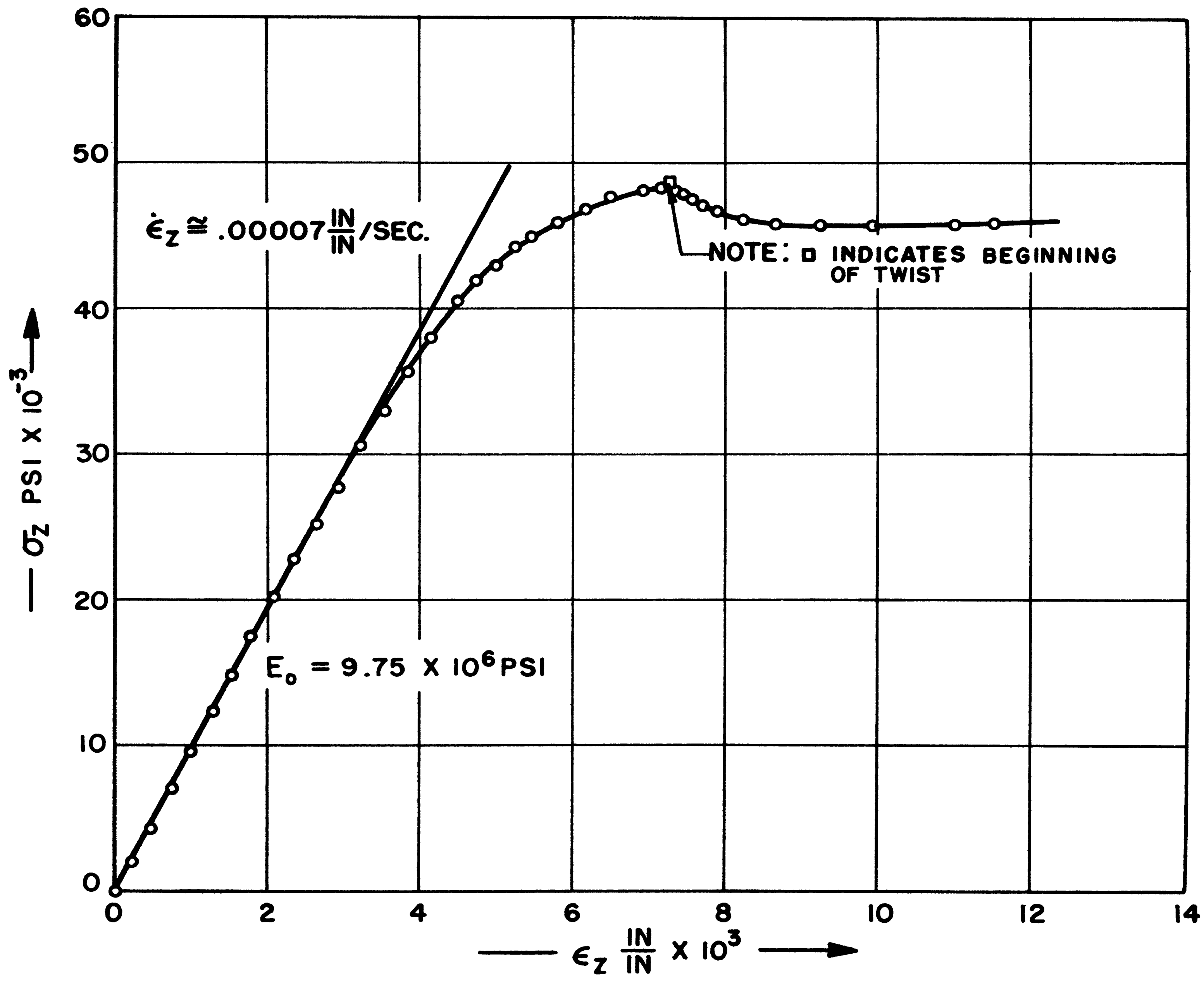

FIG. 3(a) AXIAL STRESS vs. AXIAL STRAIN
TUBE A-2 (#29)

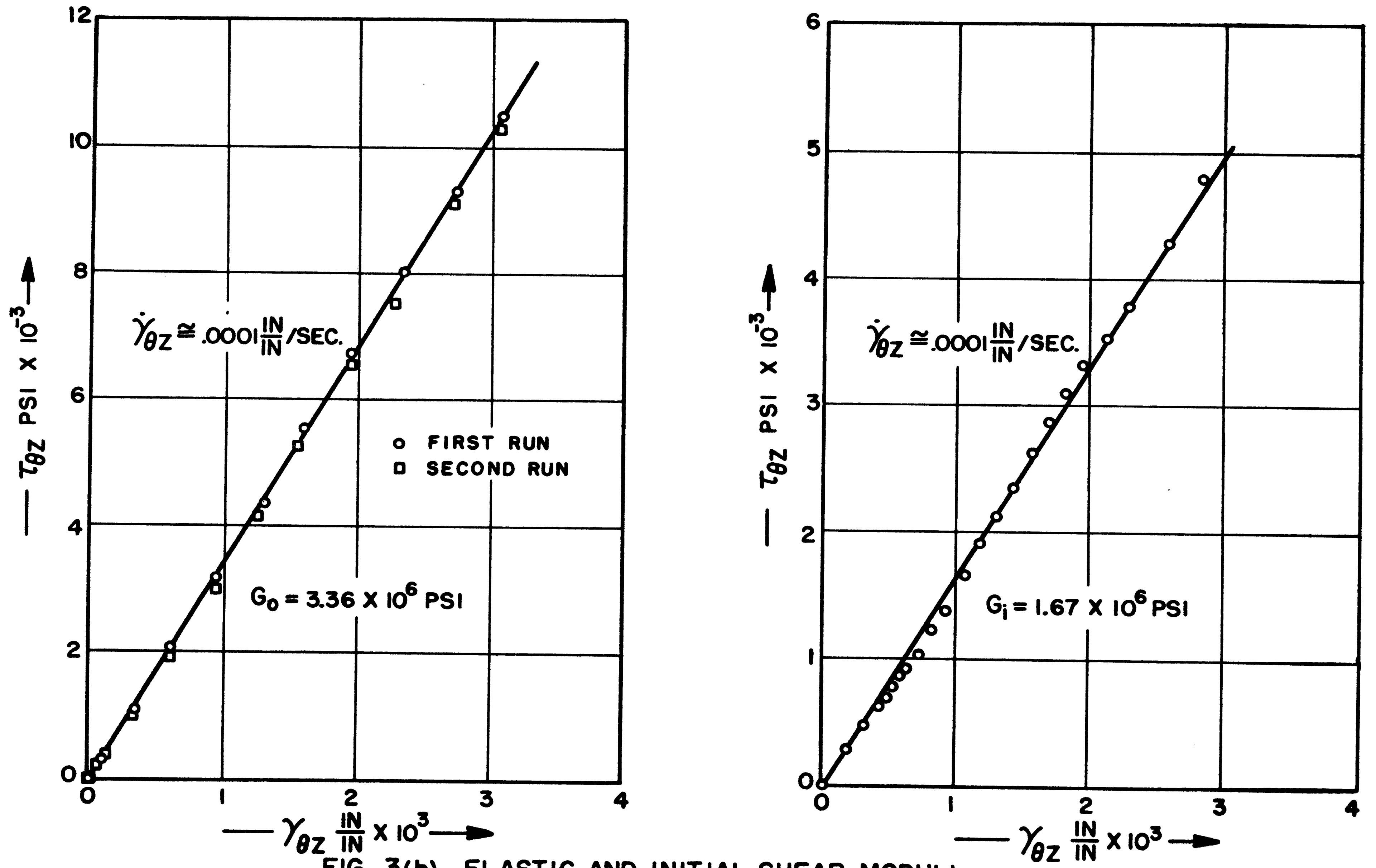

FIG. 3(b) ELASTIC AND INITIAL SHEAR MODULI
TUBE A-2 (#29)

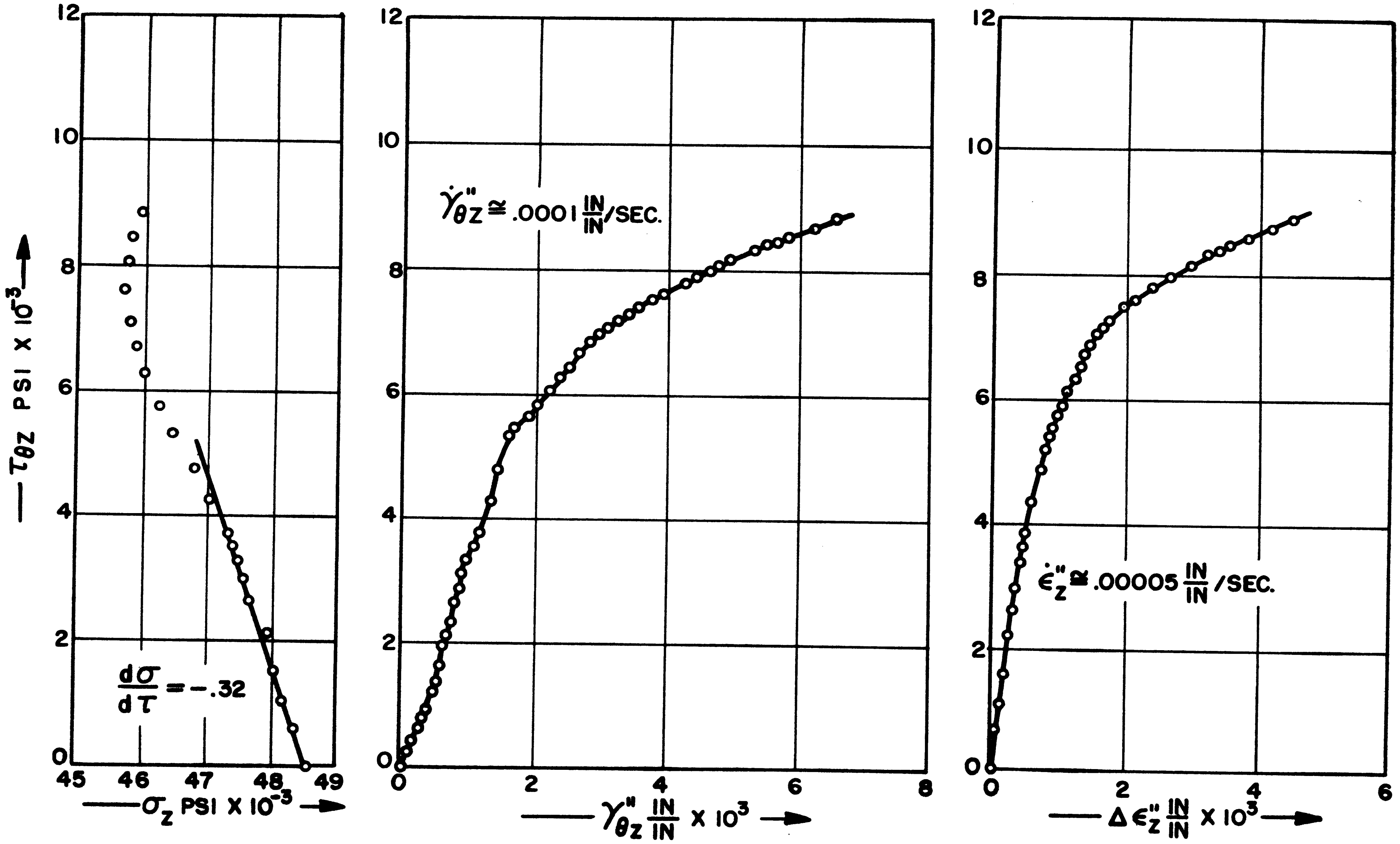

FIG. 3(c) PLASTIC STRAINS AND LOADING PATH
TUBE A-2 (#29)

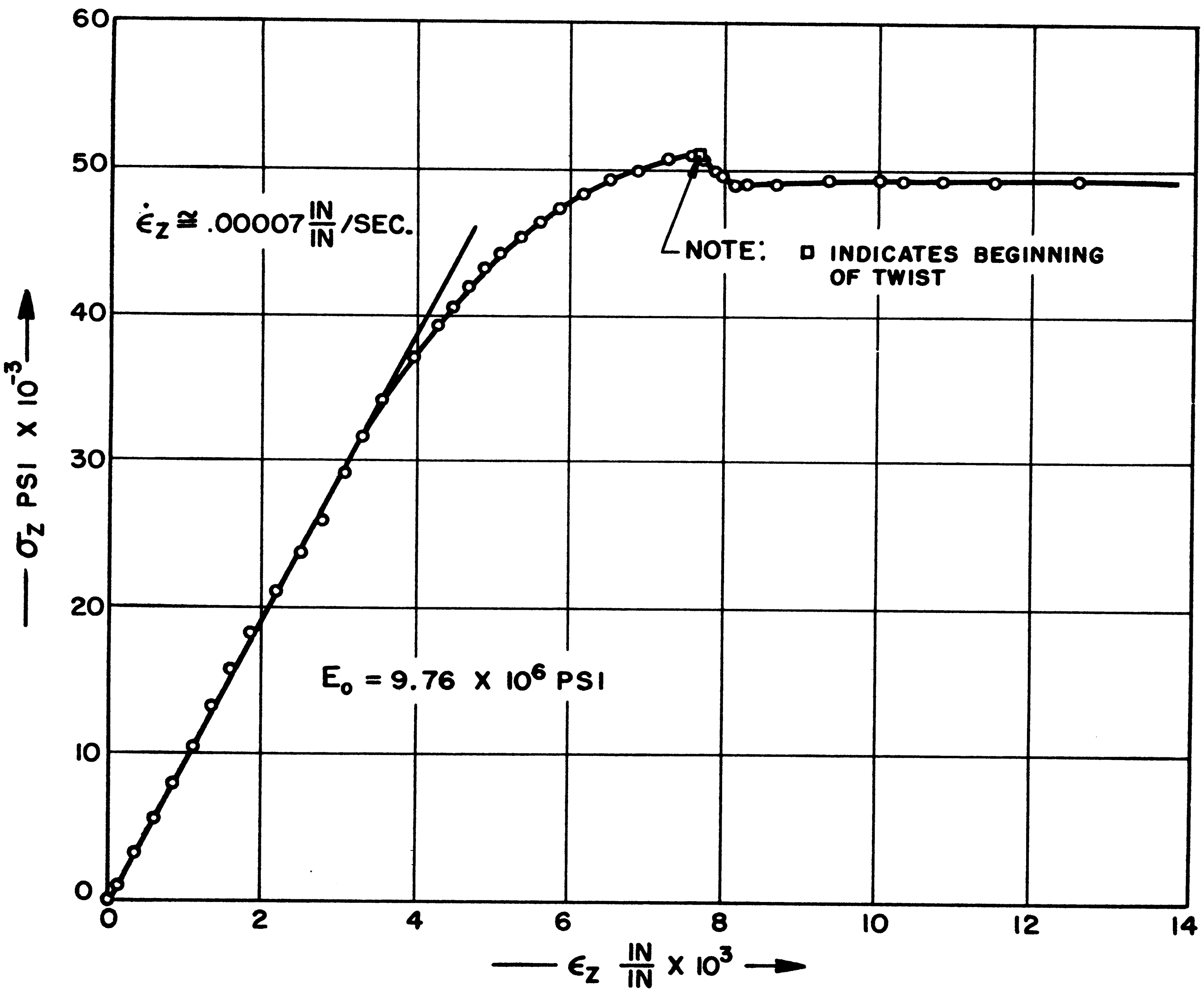

FIG. 4(a) AXIAL STRESS vs. AXIAL STRAIN
TUBE A-3 (#31)

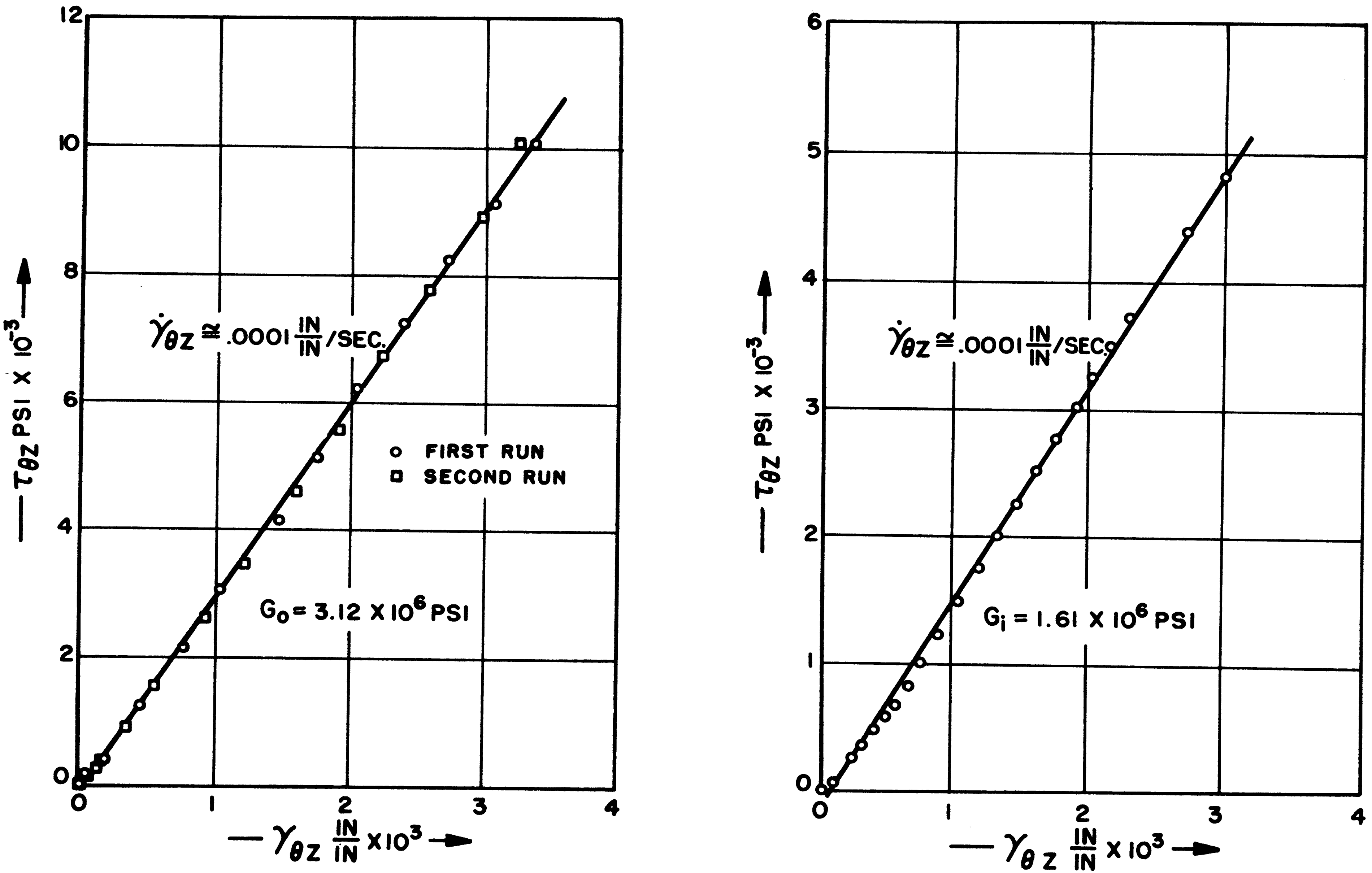

FIG. 4(b) ELASTIC AND INITIAL SHEAR MODULI
TUBE A-3 (#31)

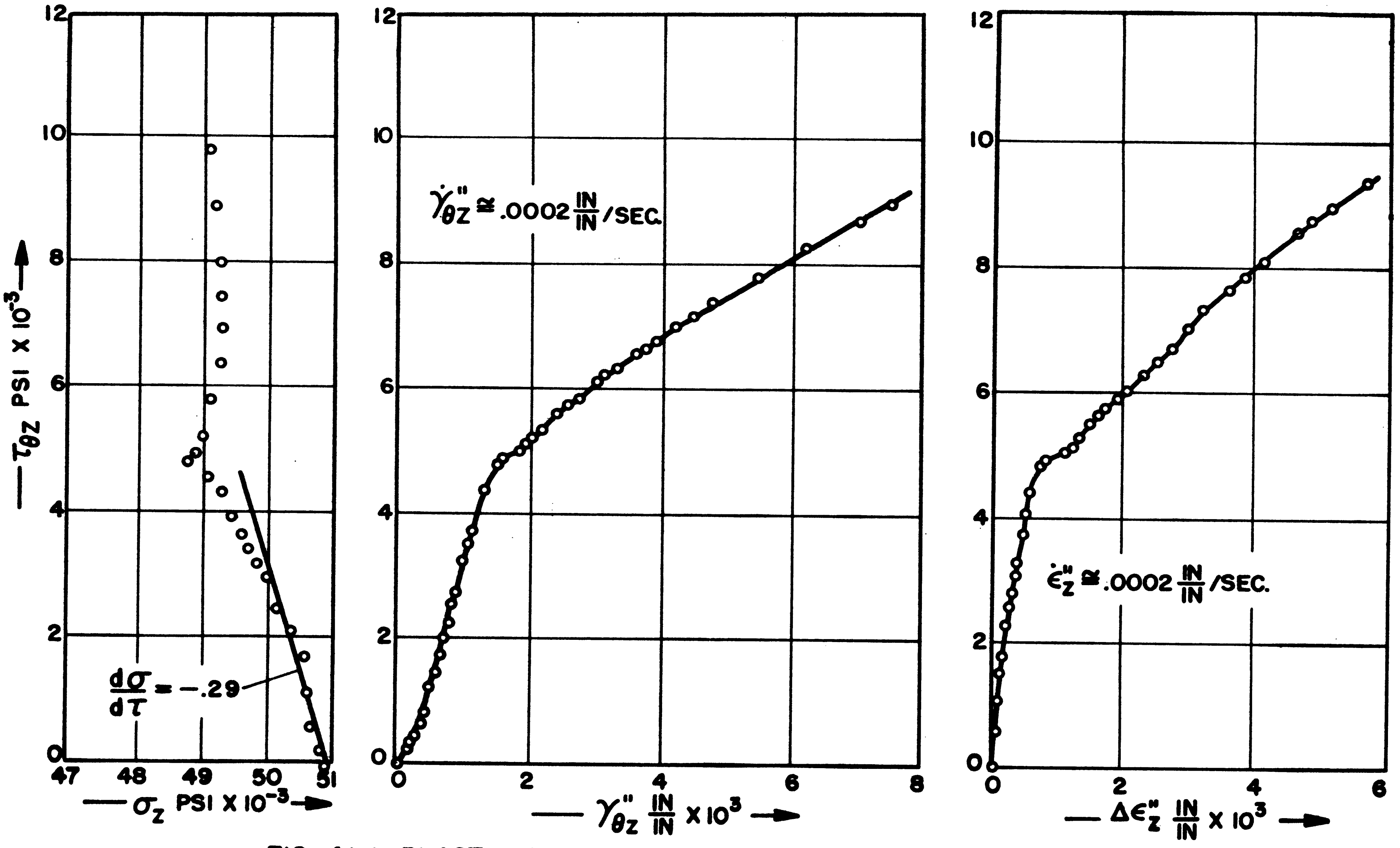

FIG. 4(c) PLASTIC STRAINS AND LOADING PATH
TUBE A-3 (#31)

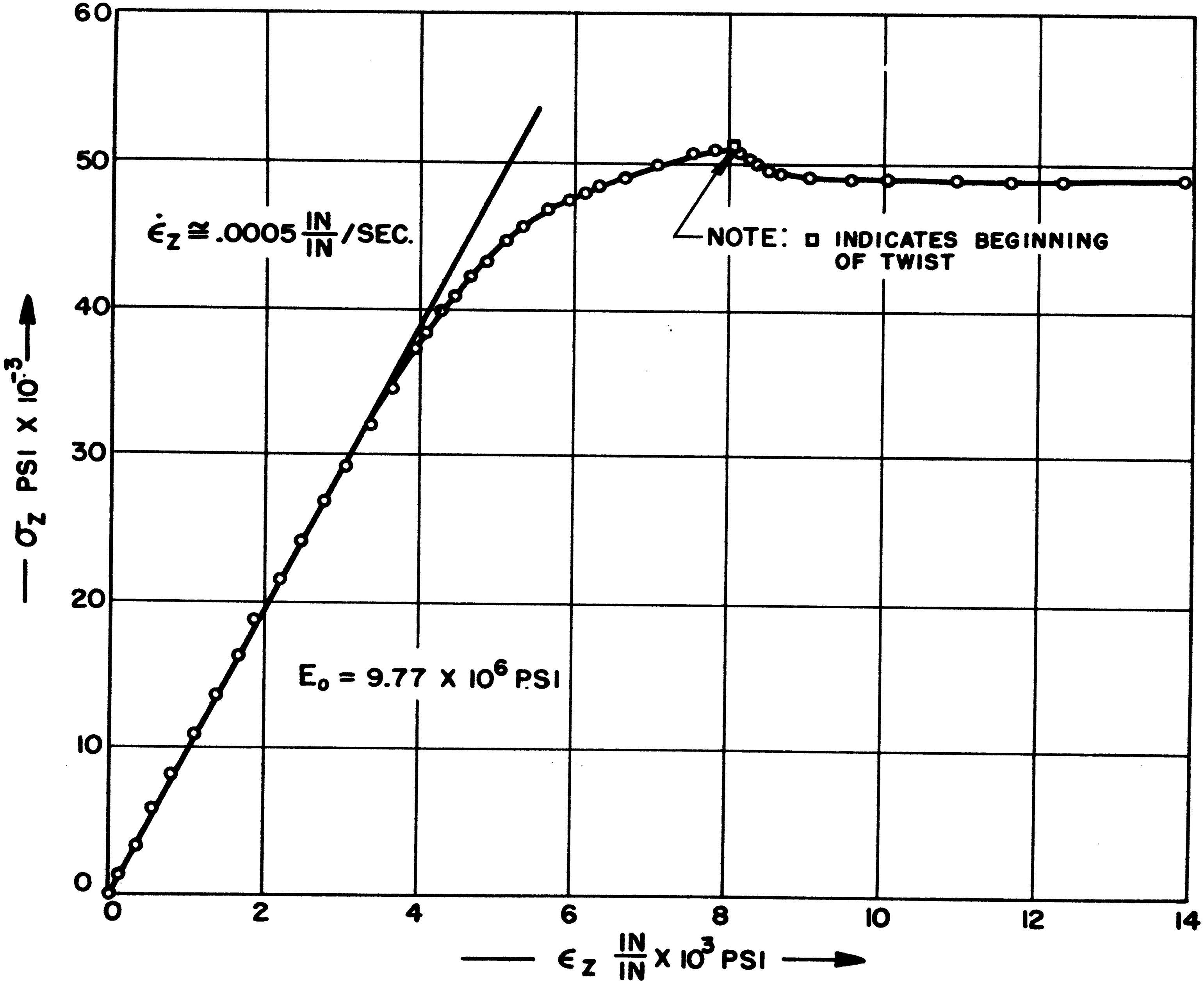

FIG. 5(a) AXIAL STRESS vs. AXIAL STRAIN
TUBE A-4 (#34)

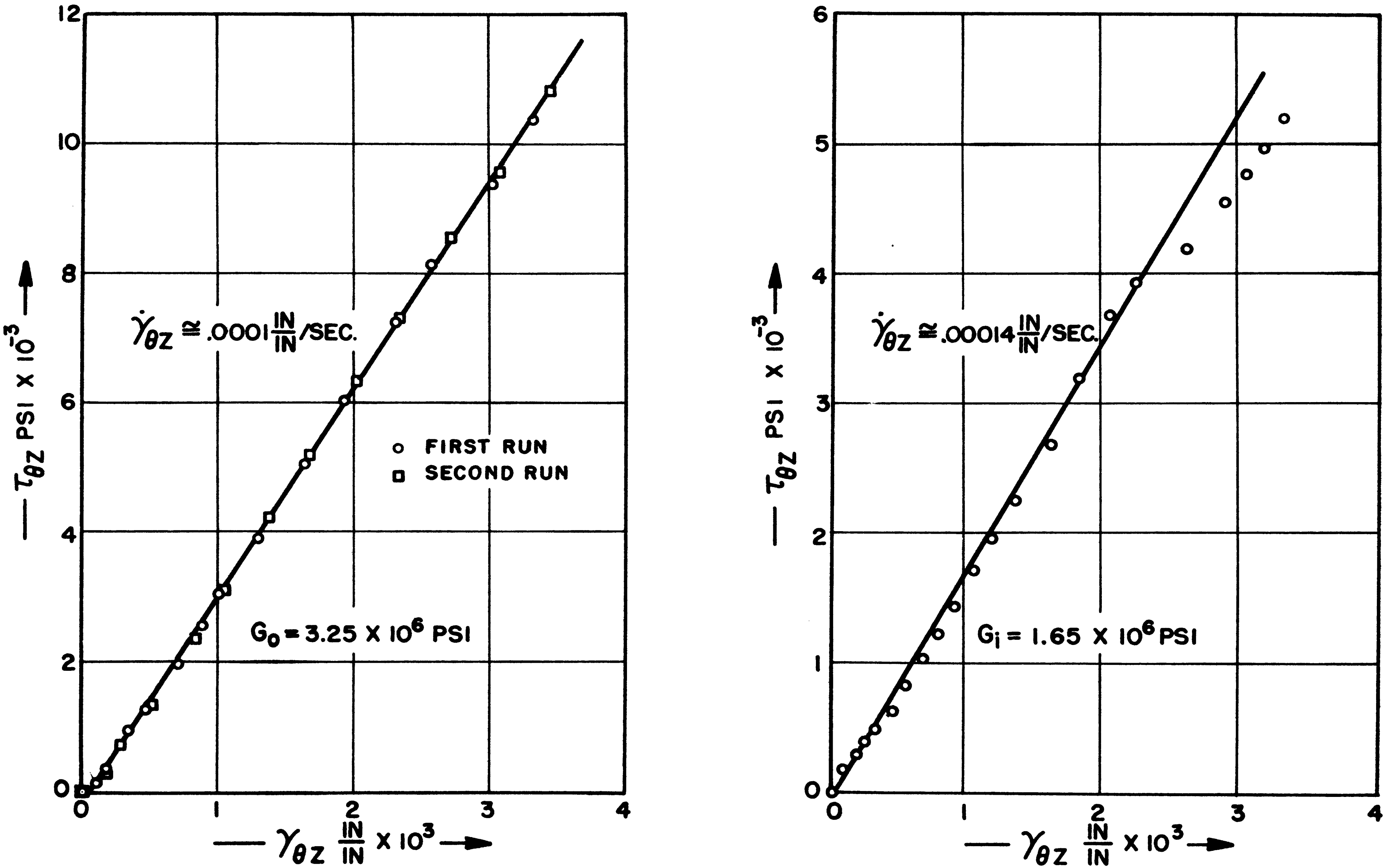

FIG. 5(b) ELASTIC AND INITIAL SHEAR MODULI
TUBE A-4 (#34)

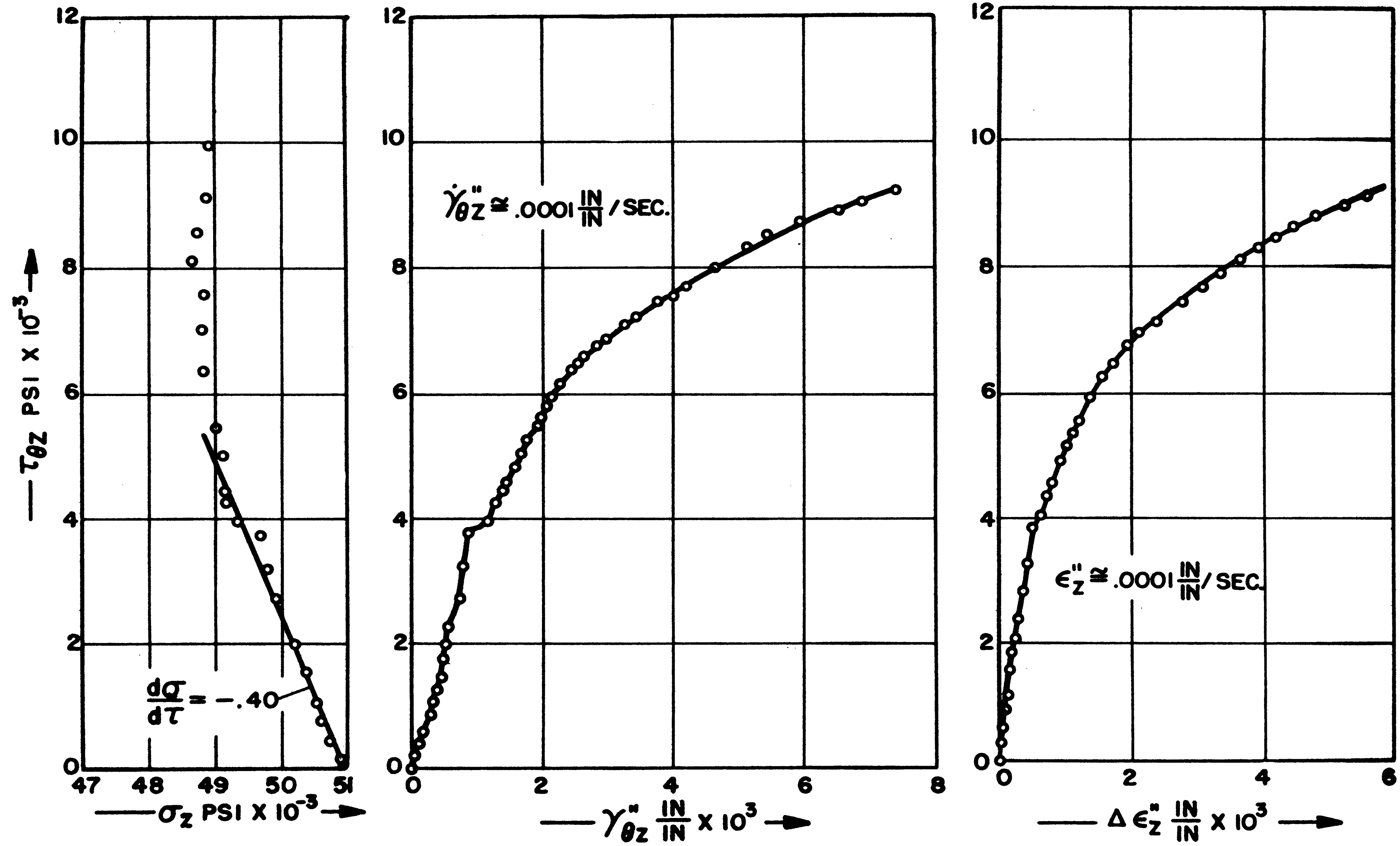

FIG. 5(c) PLASTIC STRAINS AND LOADING PATH
TUBE A-4 (#34)

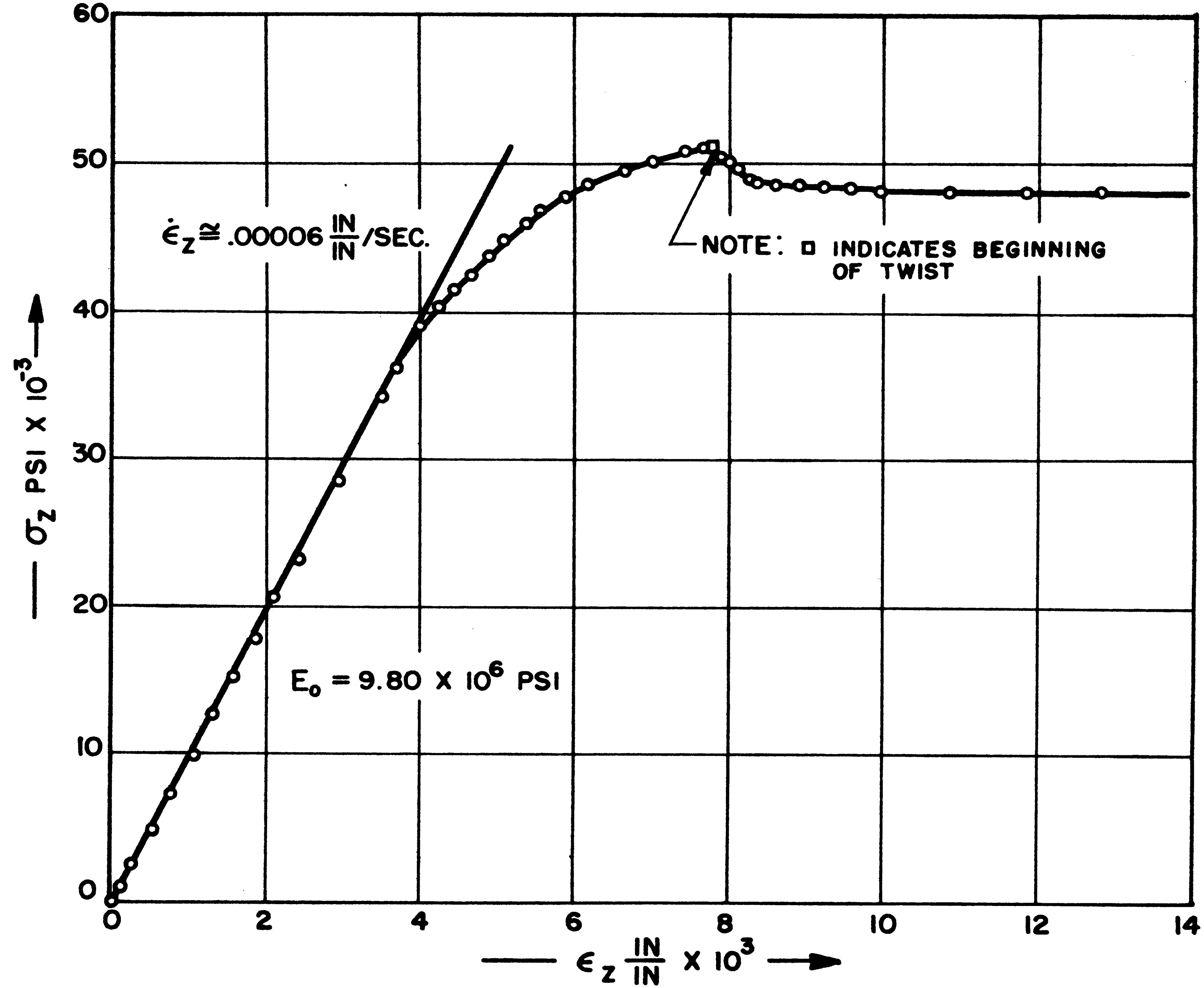

FIG. 6(a) AXIAL STRESS vs. AXIAL STRAIN
TUBE A-5 (#35)

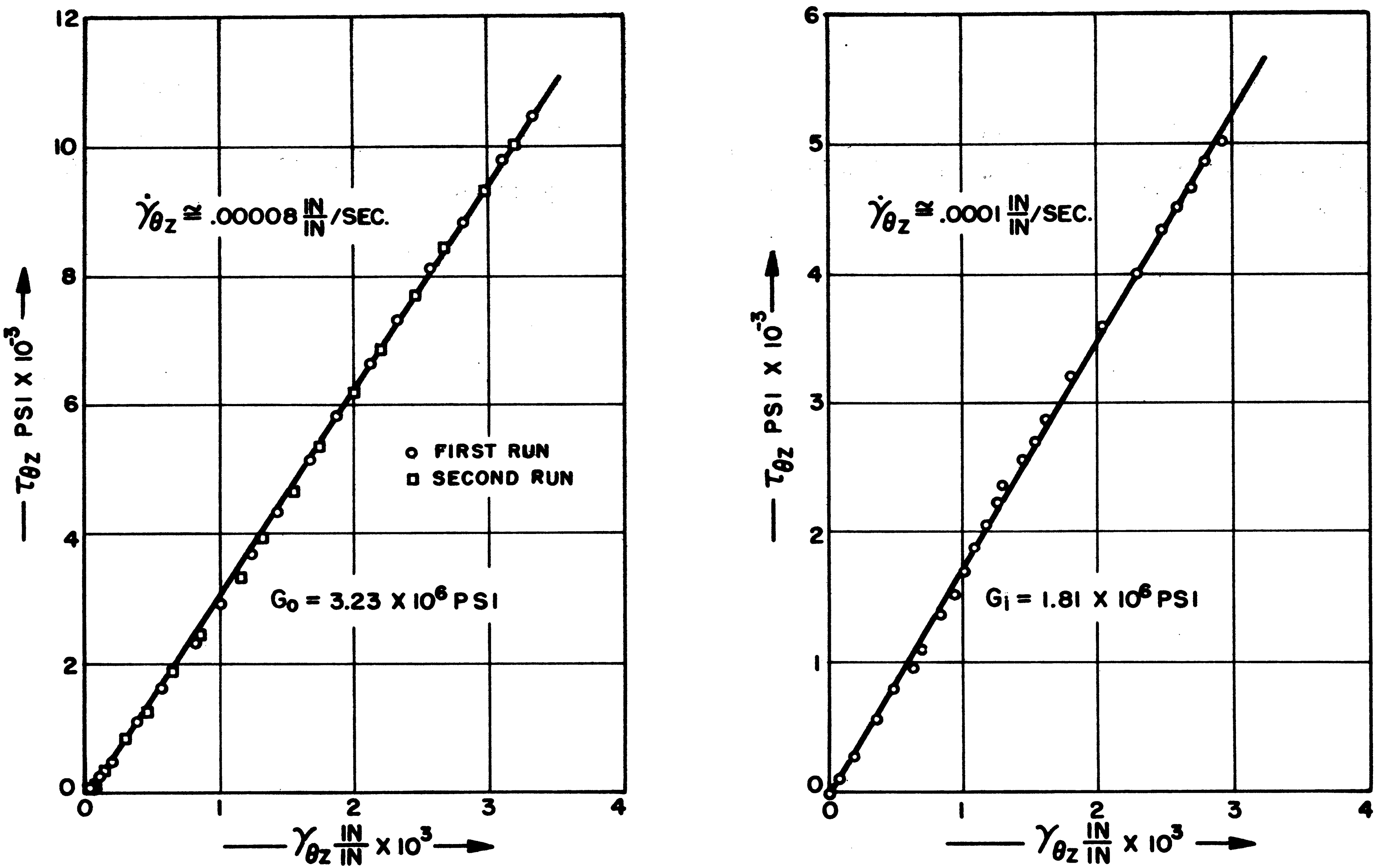

FIG. 6(b) ELASTIC AND INITIAL SHEAR MODULI
TUBE A-5 (#35)

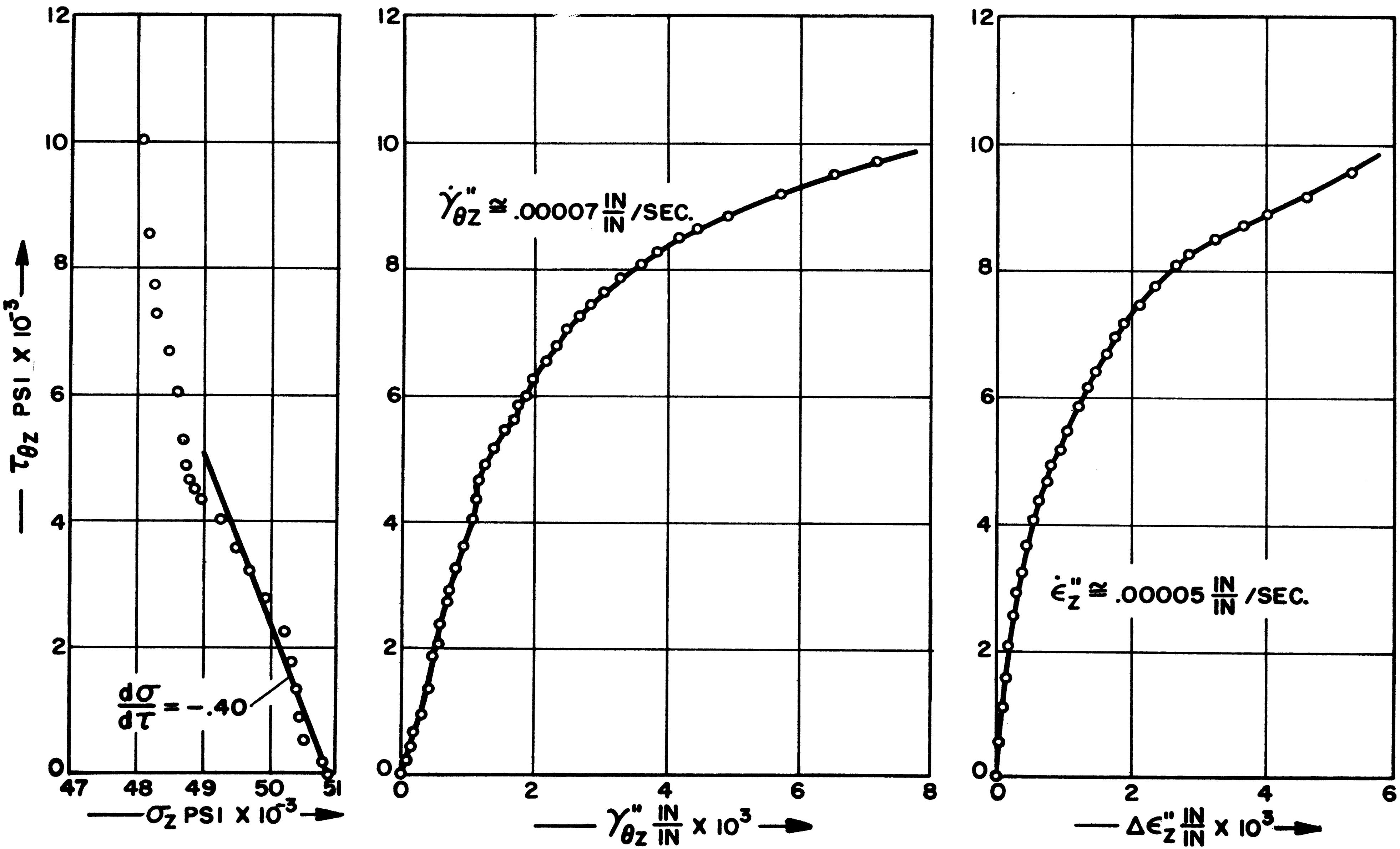

FIG. 6(c) PLASTIC STRAINS AND LOADING PATH
TUBE A-5 (#35)

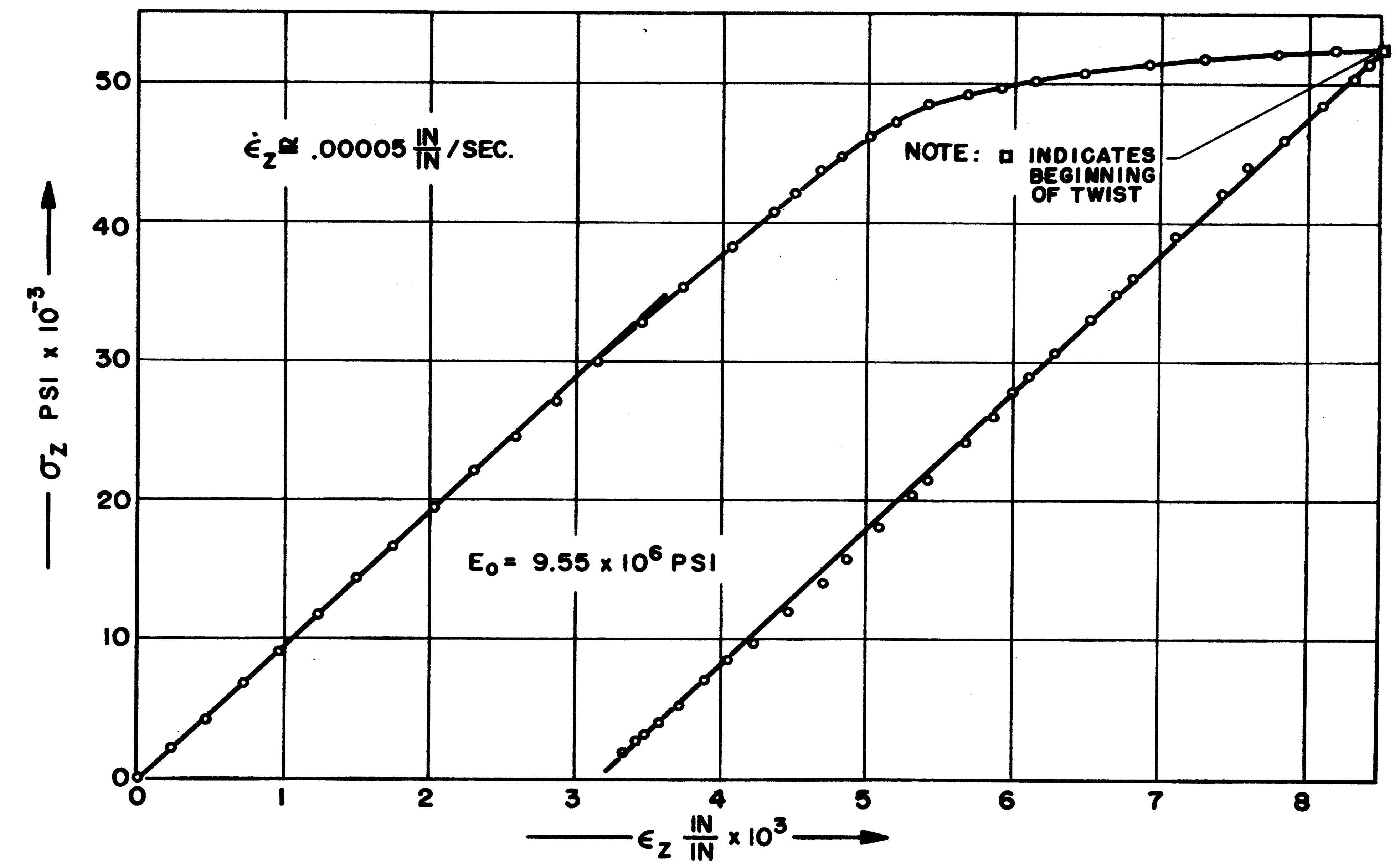

FIG. 7(a) AXIAL STRESS VS AXIAL STRAIN
TUBE B-1 (#51)

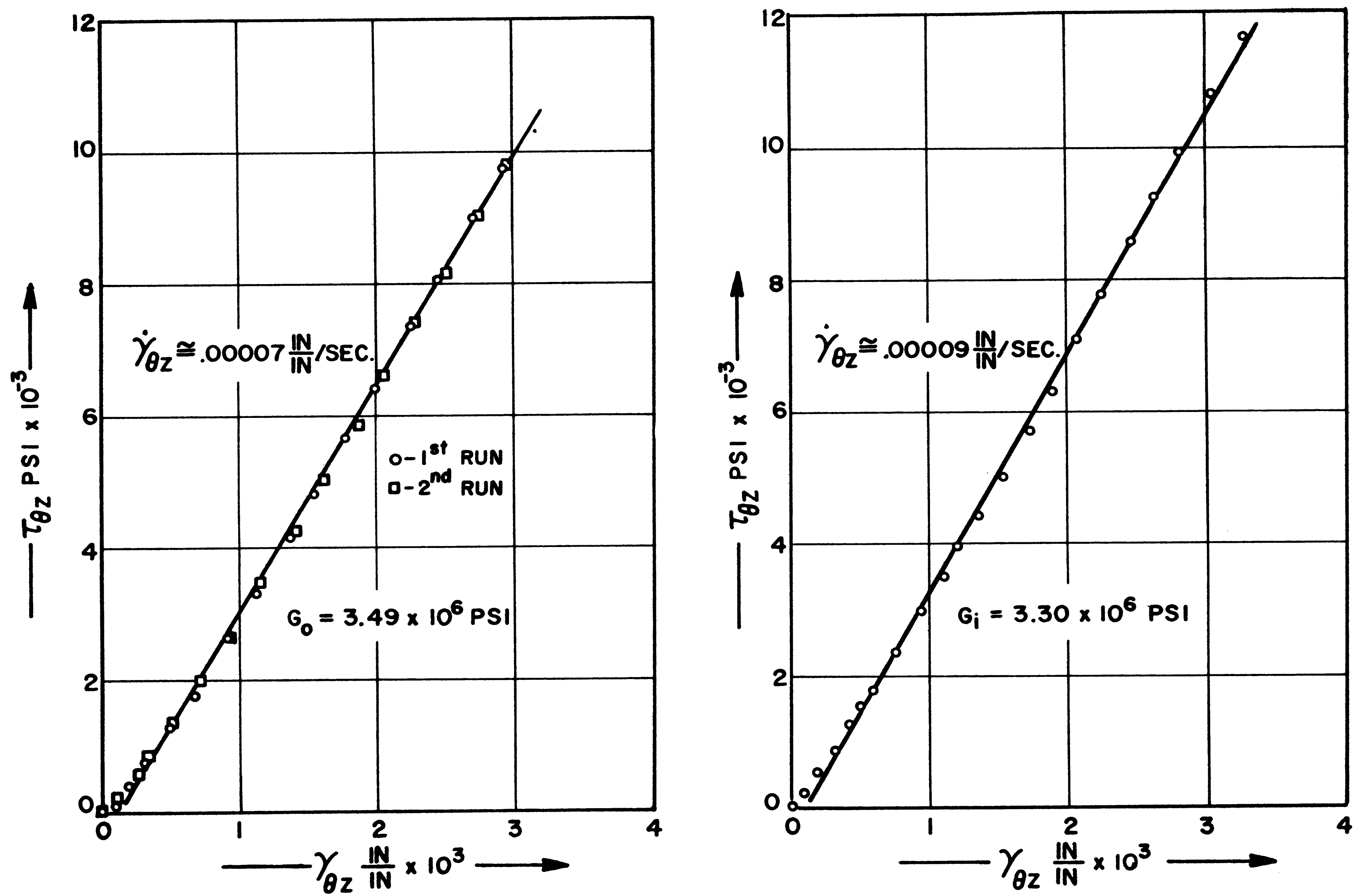

FIG. 7(b) ELASTIC AND INITIAL SHEAR MODULI
TUBE B-1 (#51)

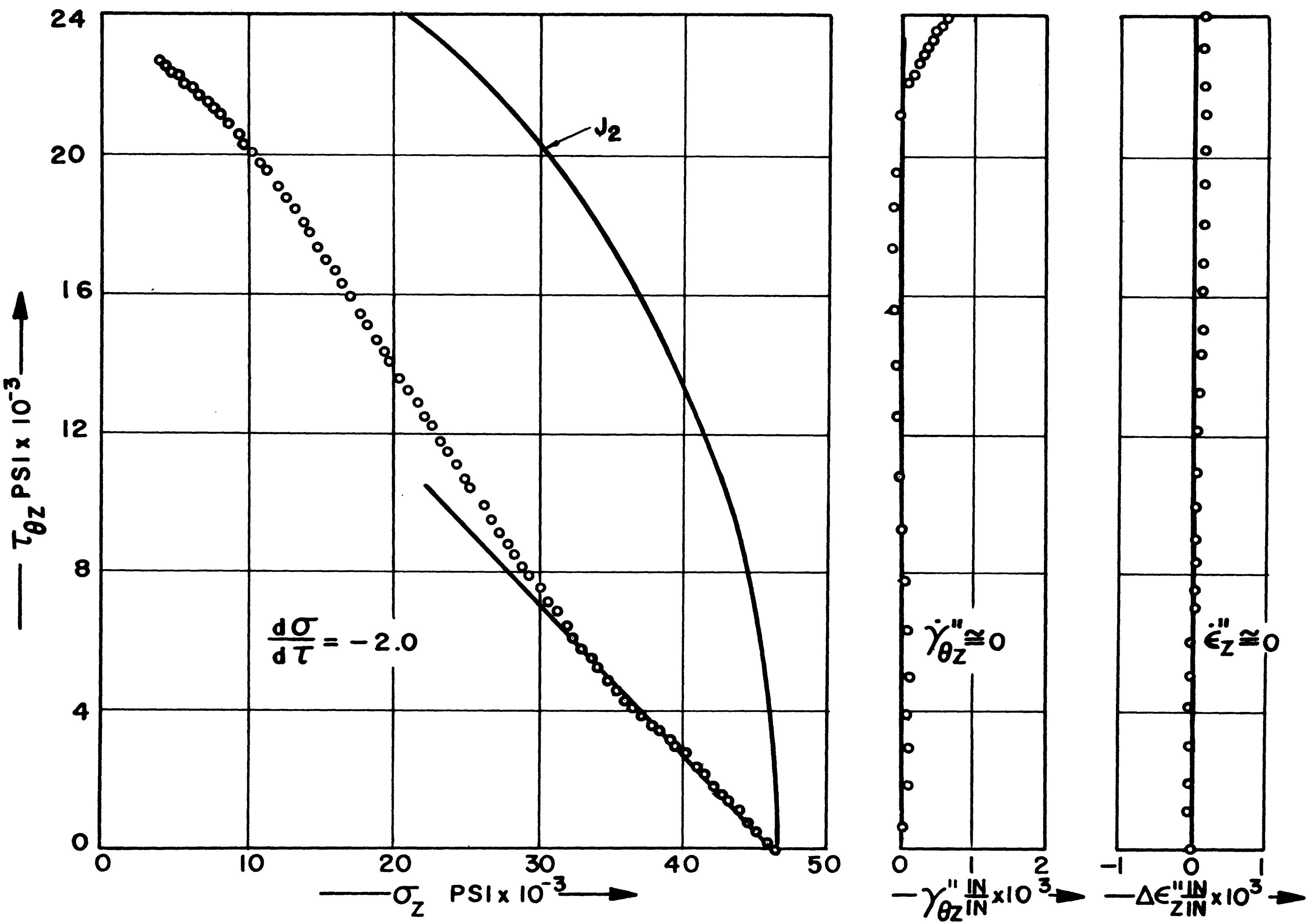

FIG. 7(c) PLASTIC STRAINS AND LOADING PATH
TUBE B-1 (#51)

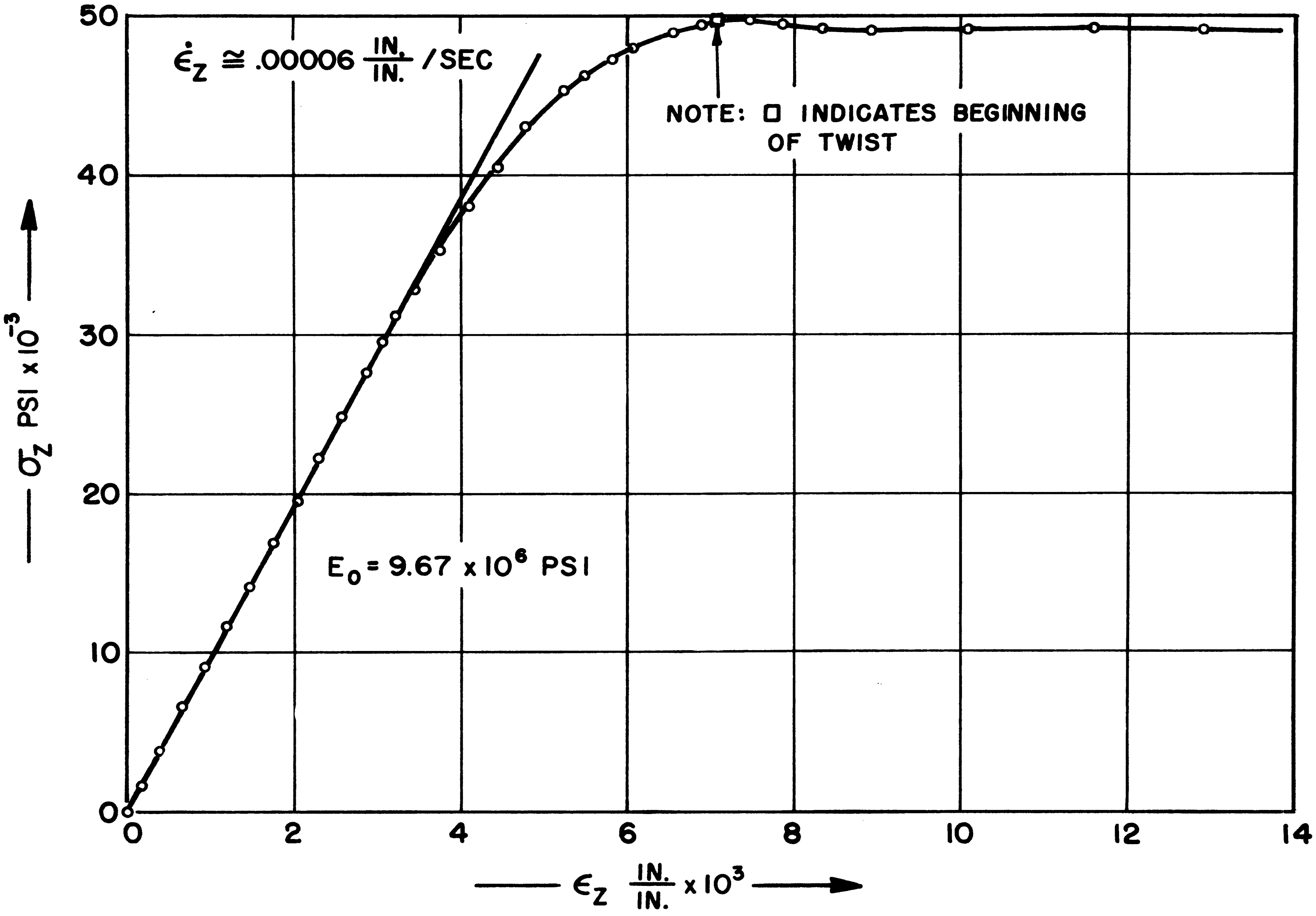

FIG. 8(a) AXIAL STRESS VS AXIAL STRAIN
TUBE C-1 (#36)

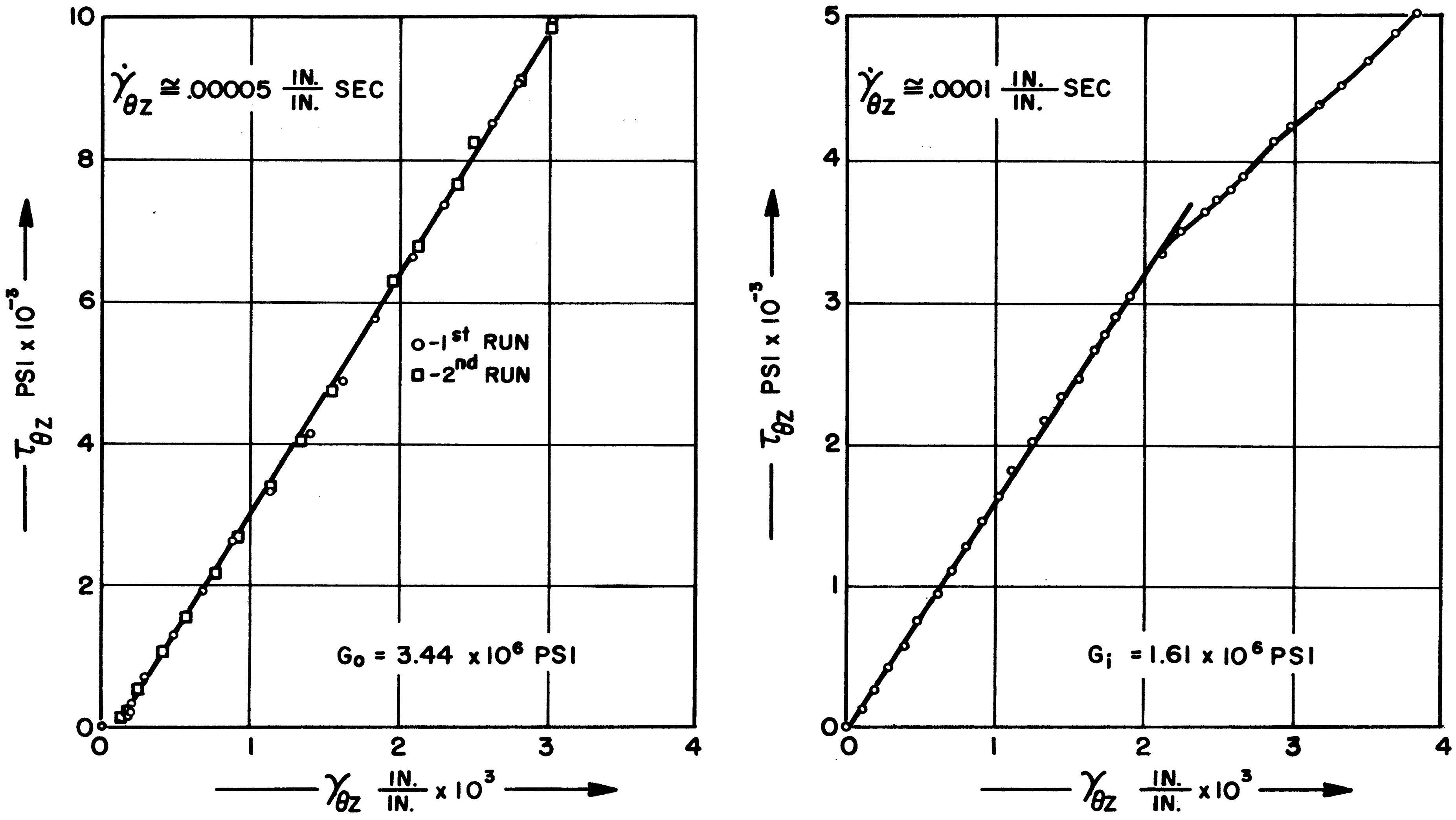

FIG. 8(b) ELASTIC AND INITIAL SHEAR MODULI
TUBE C-1 (#36)

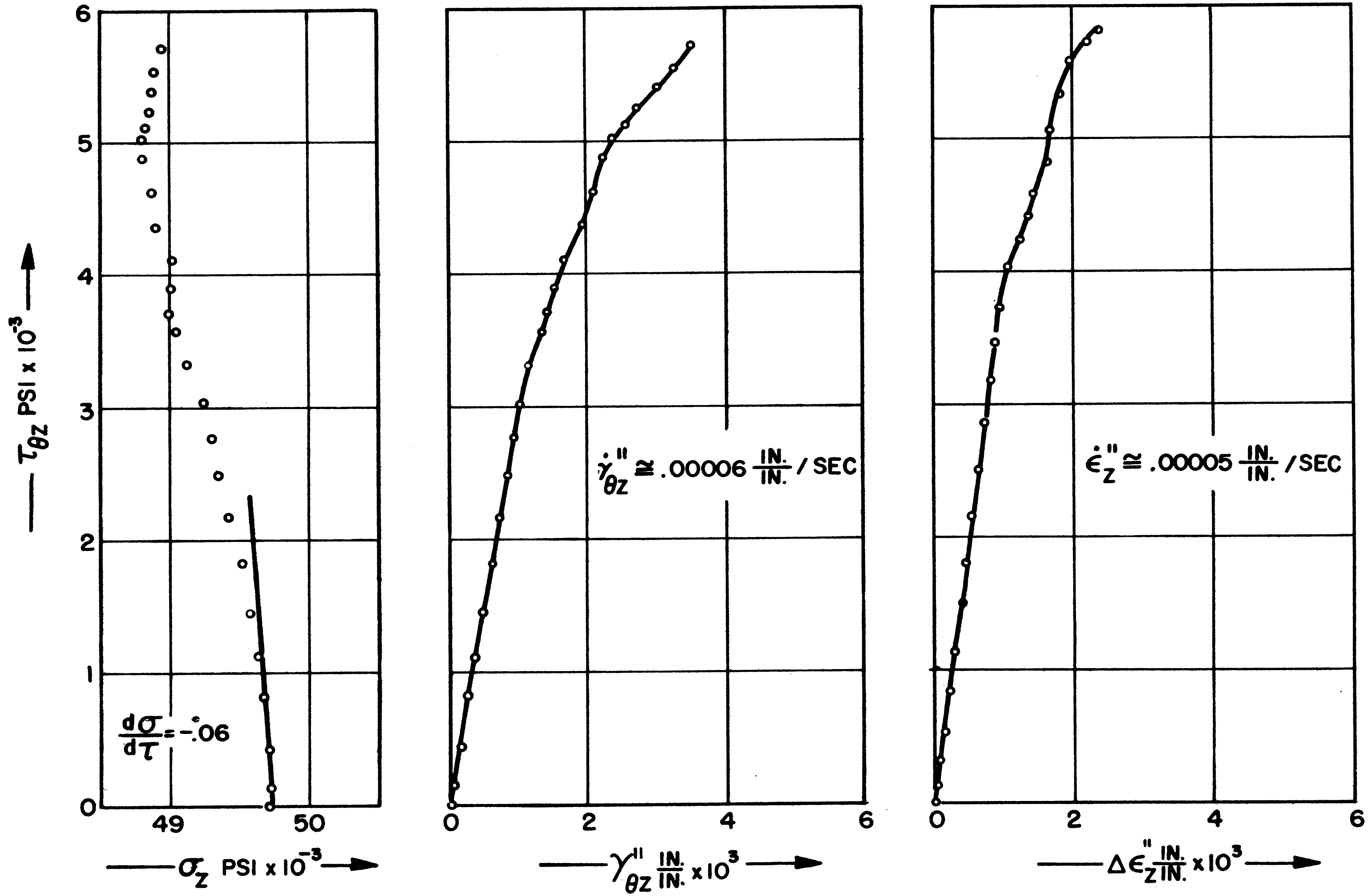

FIG. 8(c) PLASTIC STRAINS AND LOADING PATH
TUBE C-I (#36)

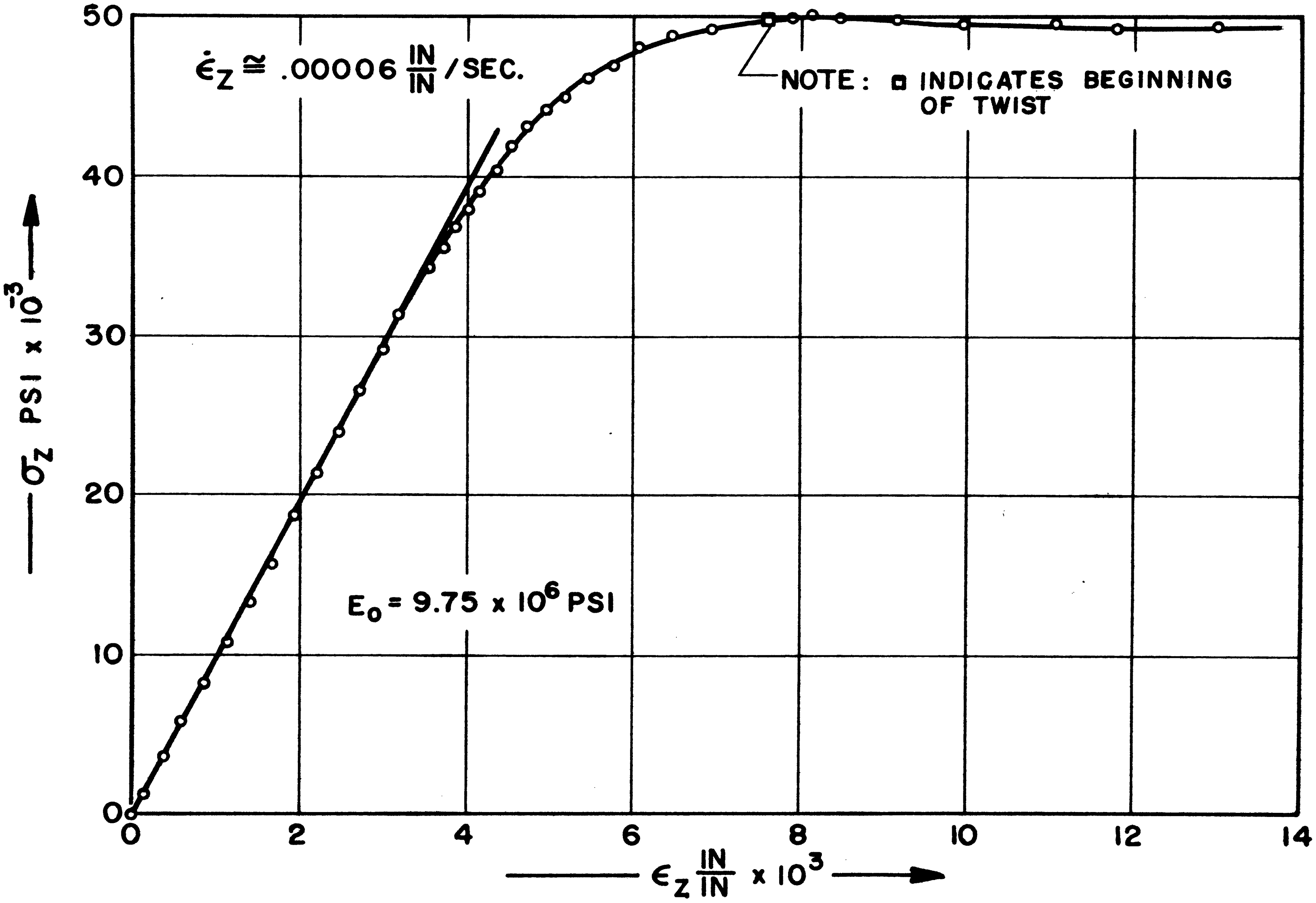

FIG. 9(a) AXIAL STRESS VS AXIAL STRAIN
TUBE C-2 (#50)

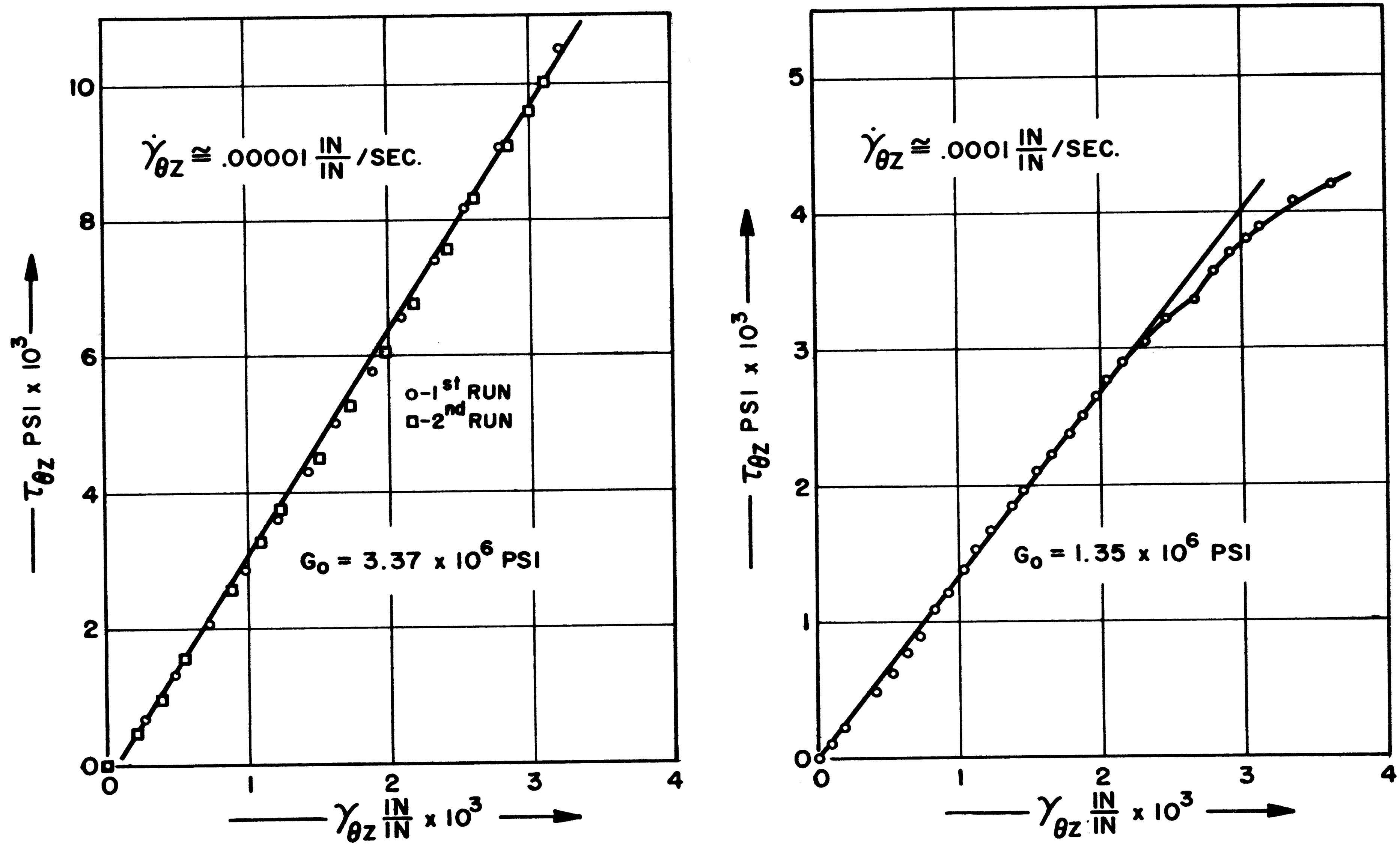

FIG. 9(b) ELASTIC AND INITIAL SHEAR MODULI
TUBE C-2 (#50)

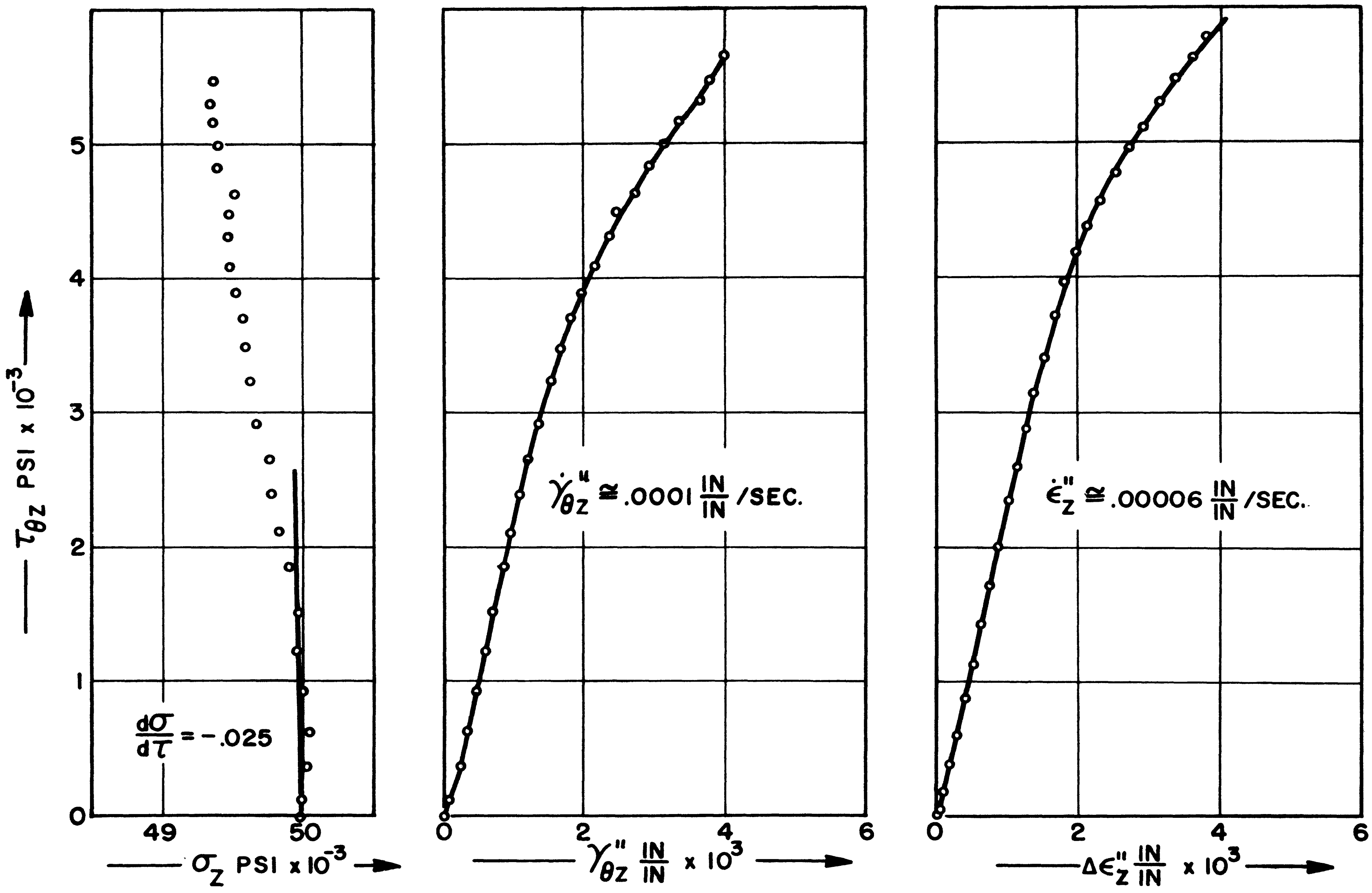

FIG. 9(c) PLASTIC STRAINS AND LOADING PATH
TUBE C-2 (#50)

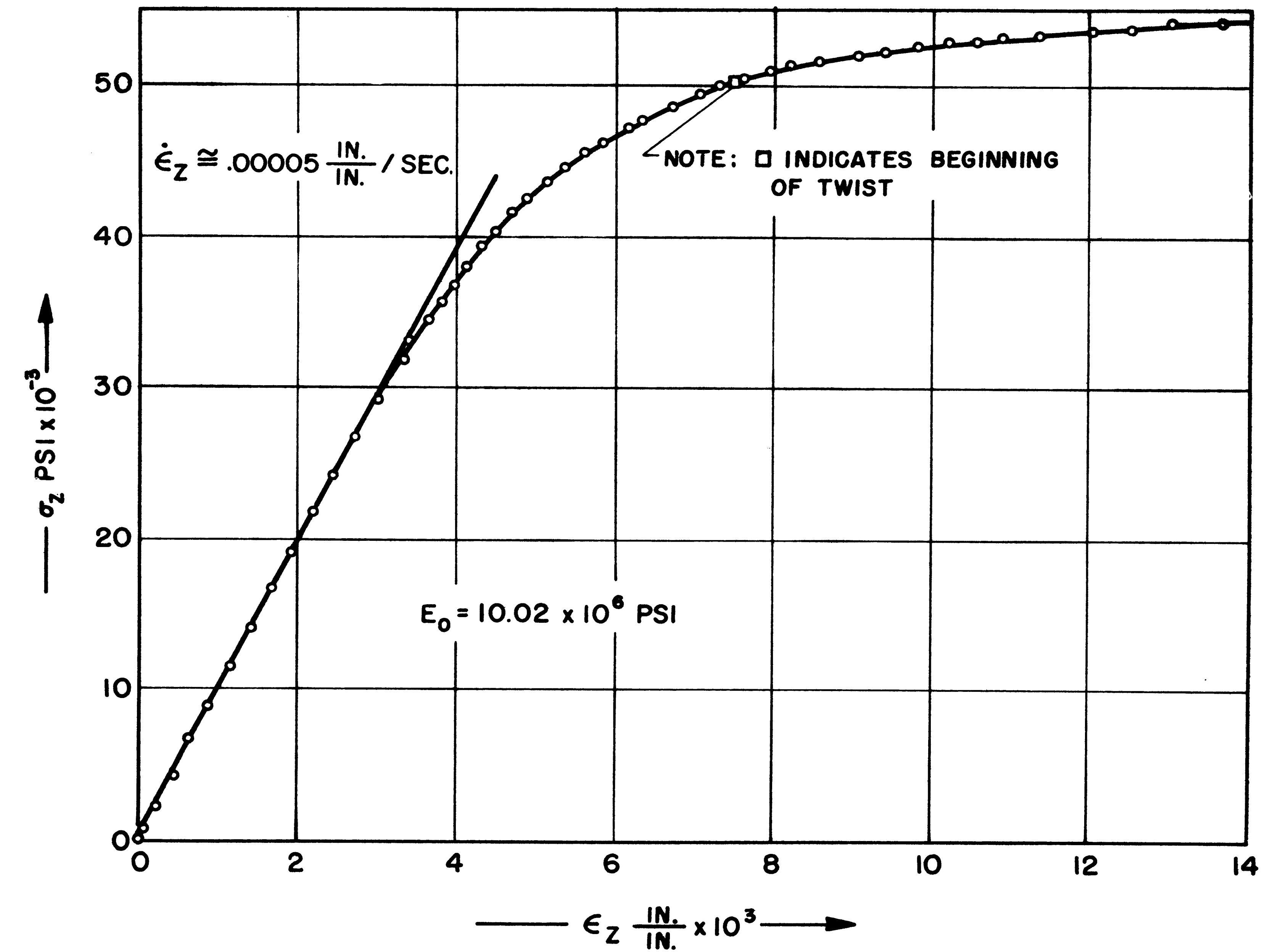

FIG.10(a) AXIAL STRESS VS AXIAL STRAIN
TUBE D-1 (#55)

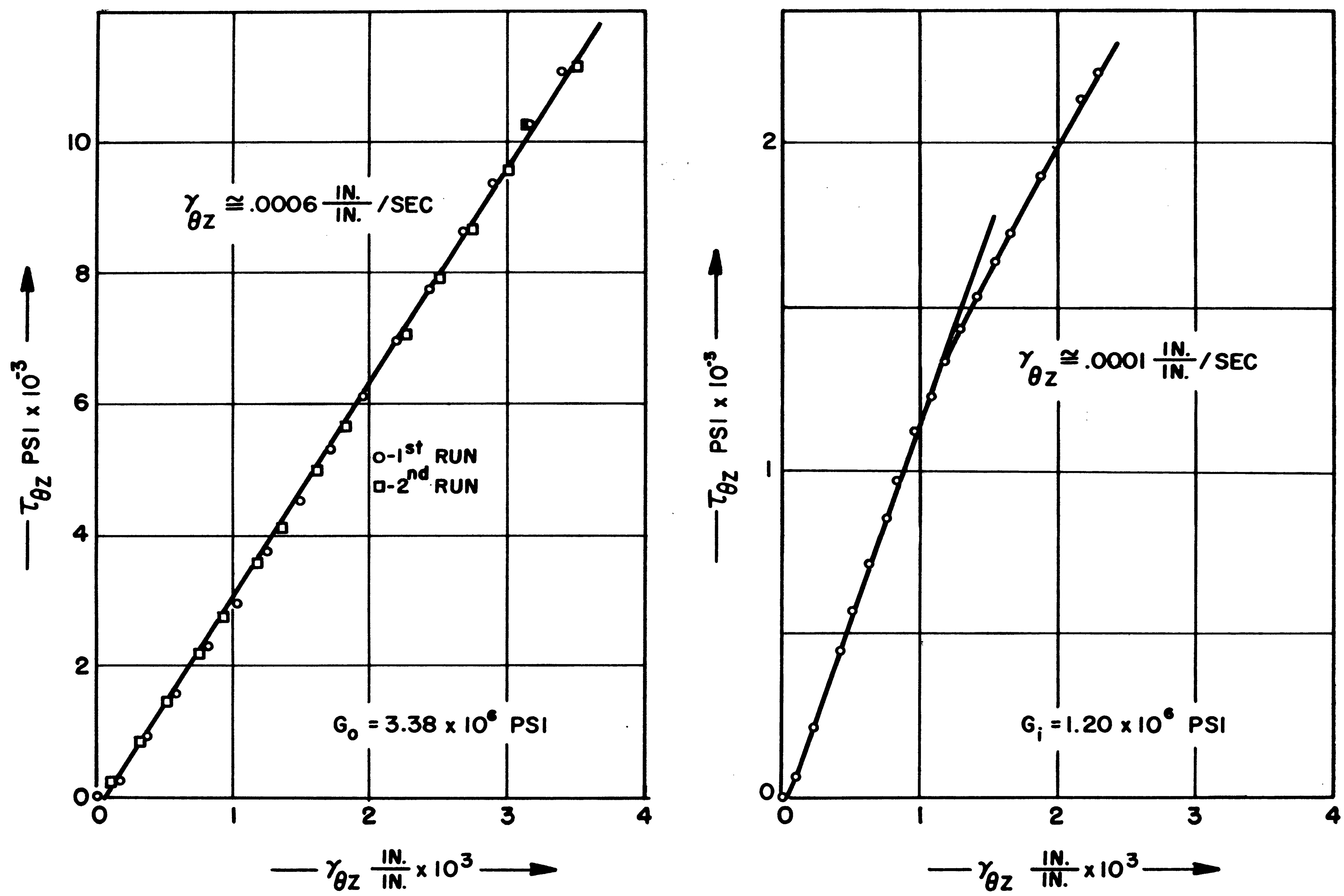

FIG. 10(b) ELASTIC AND INITIAL SHEAR MODULI
TUBE D-1 (# 55)

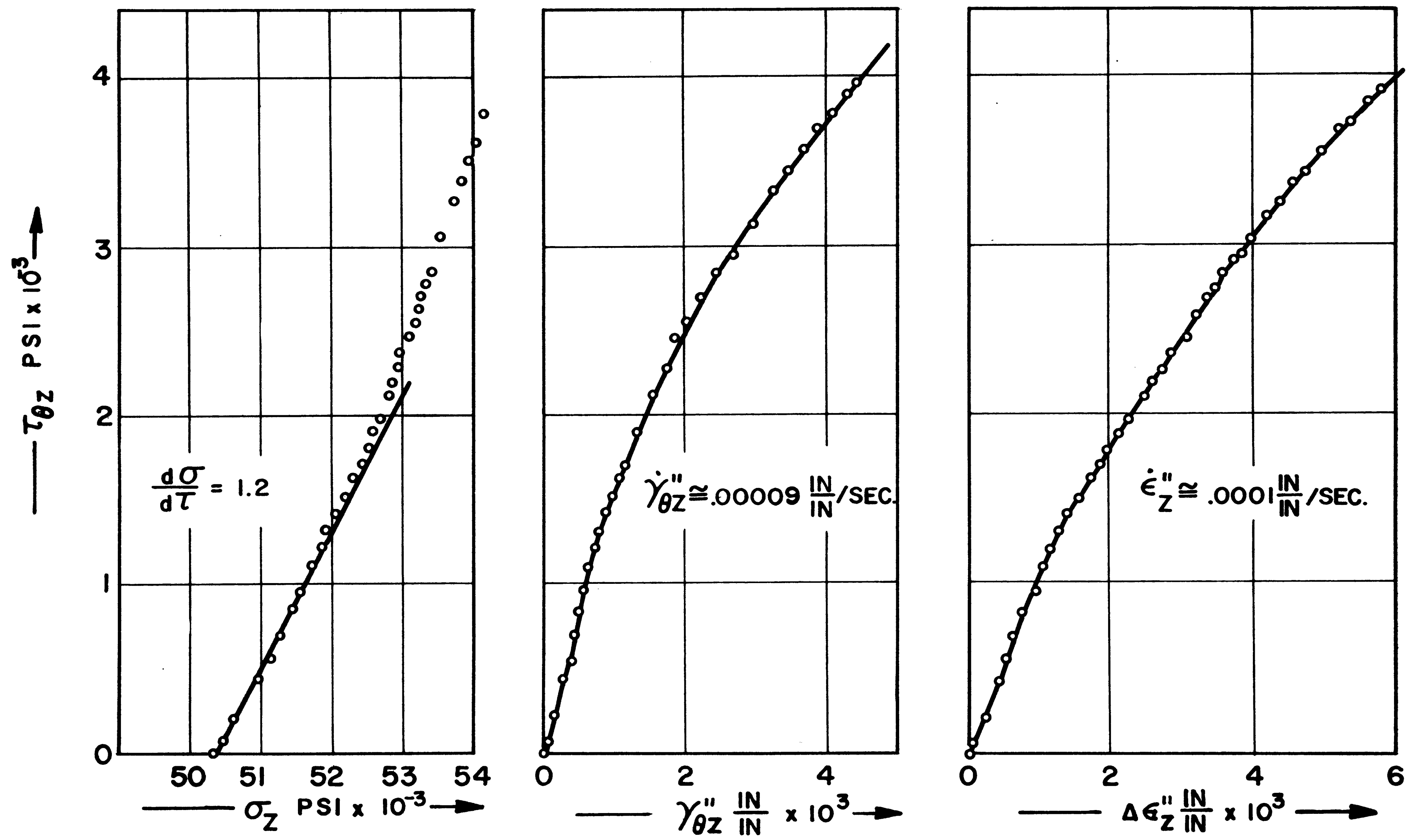

FIG. 10(c) PLASTIC STRAINS AND LOADING PATH
TUBE D-1 (#55)

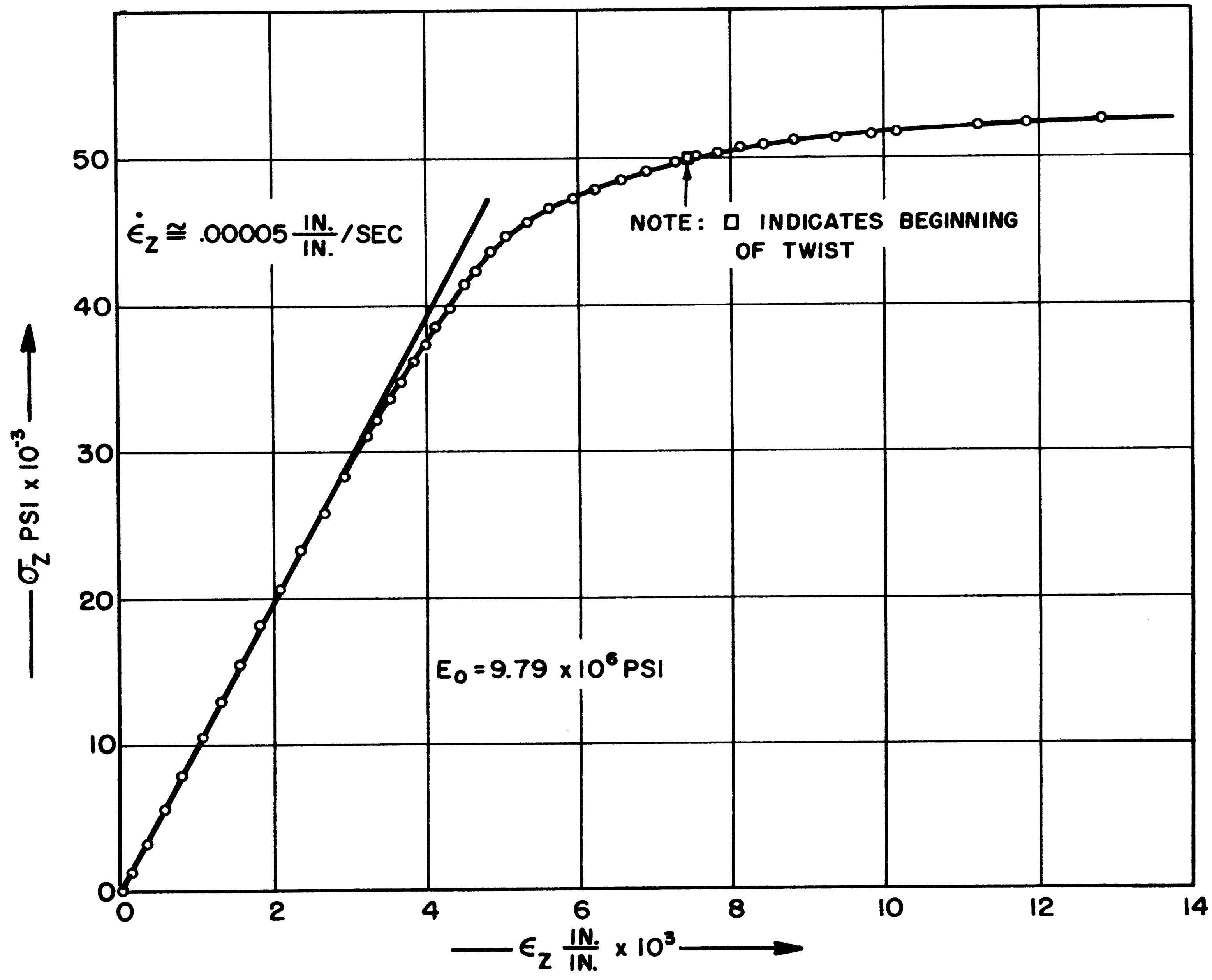

FIG. 11(a) AXIAL STRESS VS AXIAL STRAIN
TUBE D-2 (#56)

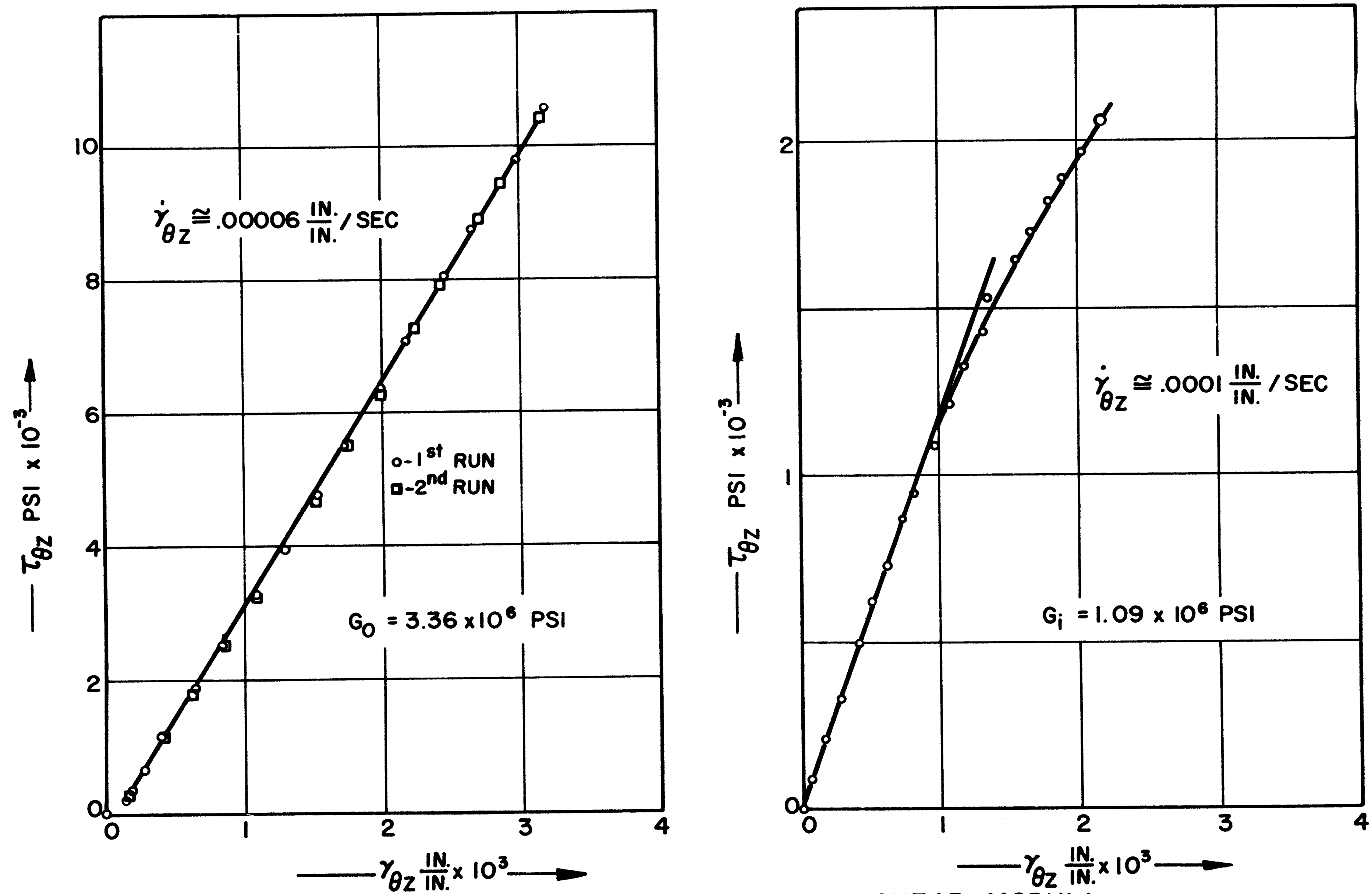

FIG. 11(b) ELASTIC AND INITIAL SHEAR MODULI
TUBE D-2(#56)

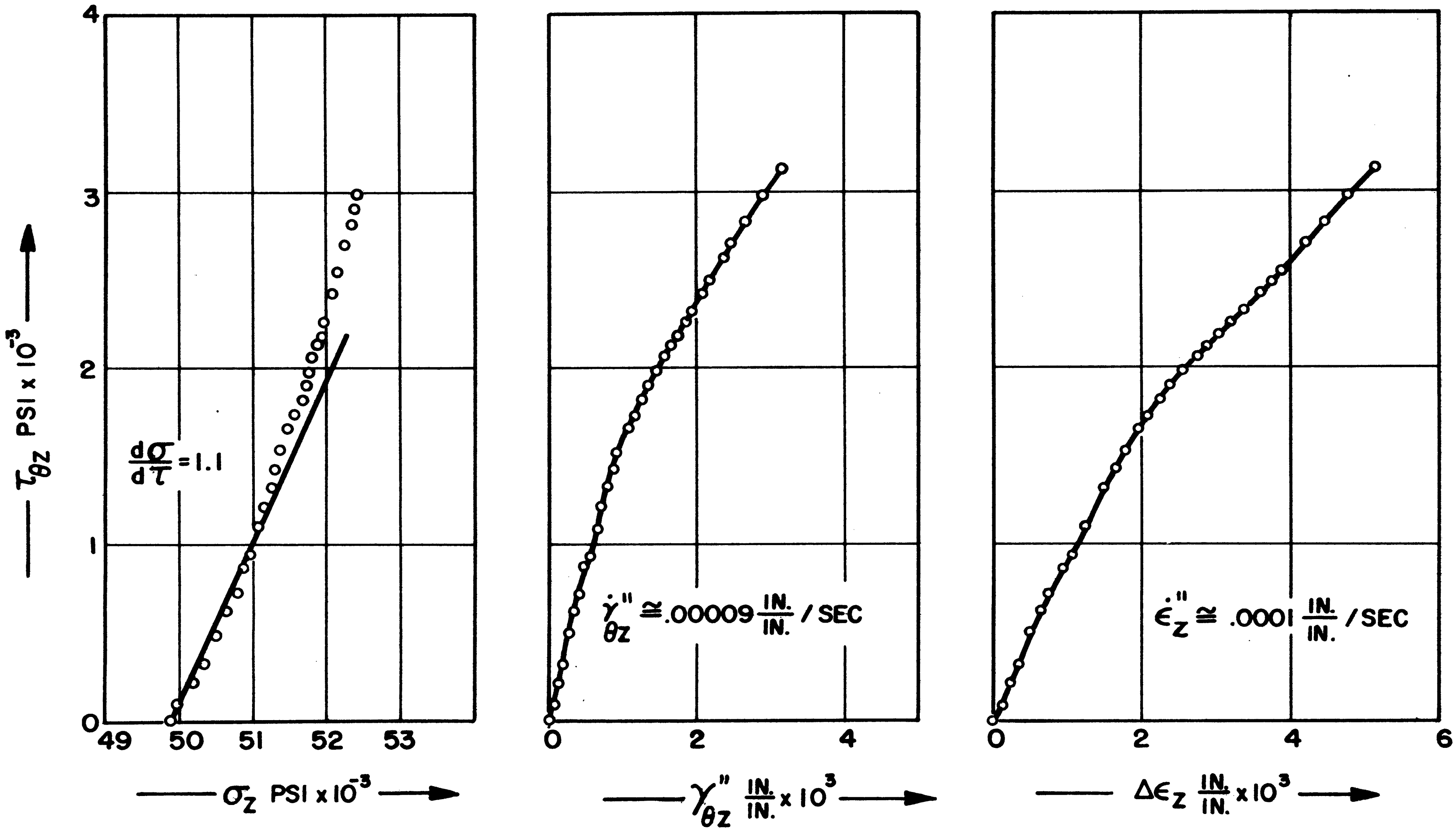

FIG. 11(c) PLASTIC STRAINS AND LOADING PATH
TUBE D-2 (#56)

Shearing strain $\gamma_{\theta z} = r \frac{\theta}{\ell_o}$ *,** ,

where θ is the angle of twist over the gage length ℓ_o .

Axial stress $\sigma_z = \frac{\text{Axial Load}}{2\pi\ (a^2-b^2)}$,

where a and b are the outer and inner radii, respectively.

Shearing stress

$$\tau_{\theta z} = G_o\, r \frac{\theta}{\ell_o} = \frac{M}{(a^4-b^4)} \left(\frac{2r}{\pi}\right)^{*} \text{(in elastic range)}$$

and

$$\tau_{\theta z} = \frac{3}{2\pi} \frac{M}{(a^3-b^3)} \quad \text{(in plastic range)} ,$$

where the torque

$$M = 2\pi \int_b^a r^2\, \tau_{\theta z}\, dr .$$

In obtaining the last formula, it is assumed that in the plastic range $\tau_{\theta z}$ is essentially uniform across the wall thickness of the tube.

A few remarks concerning the significance of the experimental results are in order before their theoretical implications can be treated. The uniformity of the specimens was very good[4]. All tubes had an 0.075-inch nominal wall thickness and 0.75-inch inside diameter, with the exception of Group D-1 and D-2 tubes, which had the same inside diameter but a wall thickness of 0.055 inch***. The anisotropy of the specimens was appreciable, as was previously noted in Reference 4; Fig. 12, showing one half of an axial cross section, is included to emphasize the severity of this condition.

The curves in Figs. 2-11 also illustrate several limitations of the experimental setup. First, a glance at the loading paths as plotted indicates the difficulty that was encountered in maintaining a linear stress path with a machine that is essentially a straining machine. Second, a slight tendency for the shear stress to lag occasionally in the initial

---

*r was assumed equal to the outer radius a of the cross section.

** $\gamma_{\theta z}$ is twice the shearing component of the strain tensor.

***See Reference 4 for design requirements on wall thickness.

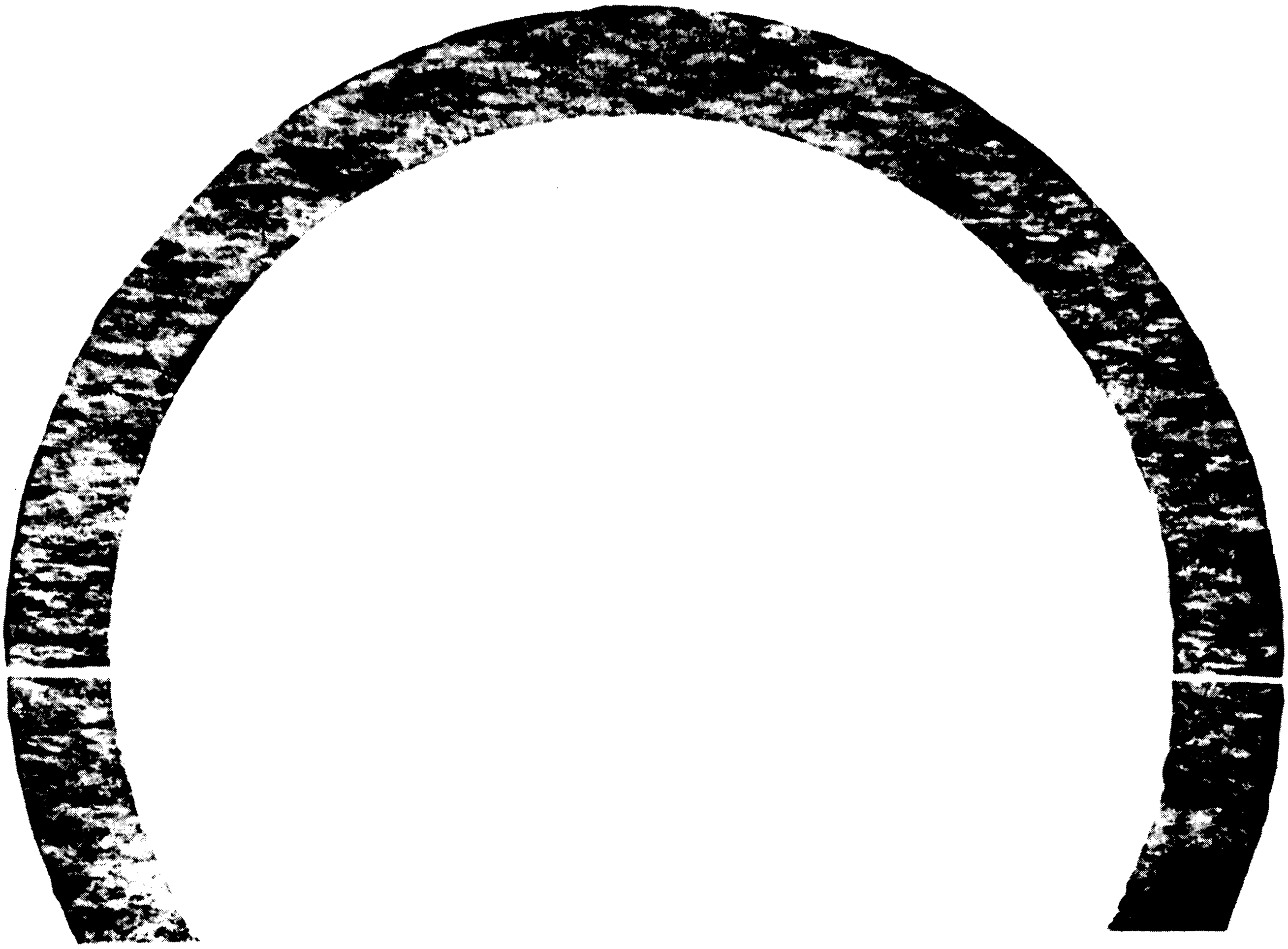

Fig. 12

portions of both elastic and plastic shear stress - shear strain curves (e.g., Fig. 7b) is a reflection of a small residual stickiness of the loading ram in the upper bearing (see Appendix of this report). Finally, the data for tube B-1, Fig. 7 afford an excellent evaluation of the small amount of interaction that remains between the axial-extension and angle-of-twist measurements. The majority of the deviations of these plastic strains from zero up until the plastic range is actually reached are probably due to this interaction. A figure of roughly ± 10 microinches can be set for the resolution of the strains and must be kept in mind in this connection.

4. Discussion

With reference to Figs. 2-11, it is seen that the repeatibility of the experimental results is good and that for Group A specimens this extends over 5 tubes. In this connection, it should be mentioned that the agreement in the values of elastic constants (Figs. 2-6) is remarkable in view of the presence of rather sévere initial anisotropy in the tubular specimens.

For Group A, the shear modulus $G_i = (d\tau_{\theta z}/d\gamma_{\theta z})_{\tau_{\theta z}=0}$ is less than the elastic shear modulus G_o (Figs. 2-6) by roughly a factor of 2. This result contradicts the predictions of both isotropic linear flow and deformation theories of plasticity and is startling, since normally, on the basis of a simple flow theory ($f=J_2$), one would assume that unloading has taken place. Apparently such a phenomenon has not been reported by previous investigators, e.g., References 13, 14, and 15. While the confirmation of this contradiction must surely be reconsidered, at present it may be attributed to several sources. These include (i) the effect of both initial and strain-hardening anisotropy and (ii) the invalidity of the usually assumed linearity of increments of plastic strain in the increments of stress.

We shall consider these possibilities separately.

(i) In discussing the influence of anisotropy, we shall accept the validity of the assumption of linearity. Consider the subsequent yield surface f_2 for an initially anisotropic strain-hardening material as shown in Fig. 13. This hypothetical loading surface is drawn so that the tangent at A (when

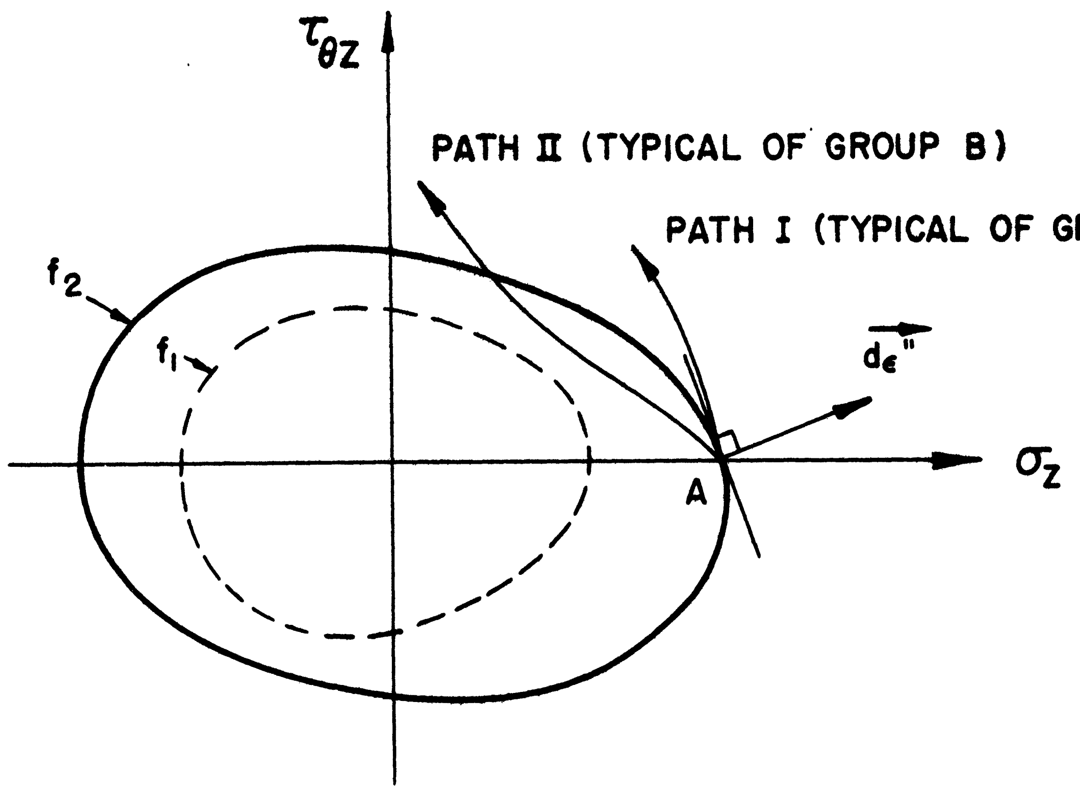

Fig. 13

traveling in a counterclockwise direction) makes an obtuse angle with the axis σ_z. Also shown in Fig. 13 are typical loading paths for Groups A and B specimens.

As pointed out by Drucker[16], when the loading surface has neither corners nor pointed vertices the increment of the plastic strain vector is normal to the loading surface. Hence, the plastic strain vector $d\vec{\epsilon}''$ at A is along the external normal to f_2 and has both axial and shearing components. Clearly then, $G_i = (d\tau_{\theta z}/d\gamma_{\theta z})_{\tau_{\theta z}=0}$ at A (beginning of twist) should not be equal to G_o. Furthermore, along the loading path I additional plastic deformation should be produced. It should be noted that had the subsequent yield surface f_2 been a blown-up version of a simple isotropic yield surface (such as J_2), then at least the initial portion of the loading path I in Fig. 13 would constitute unloading into the elastic domain. It is clear that the experimental plastic strains predicted for Group A specimens are in accord with this evaluation.

(ii) If the effects of anisotropy are ignored, then one may attribute the observed behavior of the present experimental results at least partially to the nonlinear dependence of the plastic strain increments on the increments of stress. However, on the basis of experimental evidence[17,18], it appears that the assumption of linearity is reasonable, although considerable further experiments must be performed before certainty is achieved on this matter.

With reference to Fig. 13, if the loading path is as in Group B, then G_i would be expected to have the elastic value G_o, considering that unloading has definitely occurred. That this is indeed the case can be seen from Fig. 7, where $G_i \simeq G_o$. The small amount of deviation in these values is not unreasonable, in view of the presence of anisotropy.

For Groups C and D, where loading would normally be assumed to occur, the existence of plastic strains after the application of torque is verified. These results are also in accord with the above speculation. Again, the value of G_i for these groups is about 1/2 of G_o, contrary to the results predicted by isotropic theories of plasticity.

It is the opinion of the present authors that the experimental results given here are explained in the main by the presence of initial and strain-hardening anisotropy. It may, of course, be possible that other factors such as strain rate and time effects, grain size, homogeneity of stress state, and machining of specimens may have influenced the results. However, these effects are felt to be small and only a comprehensive experimental investigation could evaluate their influence.

Aside from the initial value of the shear modulus G_i and its consequences discussed above, the general trend of the results agrees favorably with those of other investigators[13]. Comparisons between experimentally determined plastic strains with those predicted by simple flow and deformation theories are not plotted in Figs. 2-11 since, in view of the discussion concerning the effects of anisotropy on the yield surface, such comparisons appear to be useless. However, it might be of interest to compare the results given here with the predictions of a slip theory of plasticity[9].

5. Conclusion

An experimental technique has been developed to pursue investigations in plasticity. This method, which permits combined tension-torsion experiments, has been shown to give good repeatibility.

Experimental results for 10 tubular specimens of an aluminum alloy (24S-T4), in which torsion was followed by tension, are presented. These results are discussed in the light of the fundamentals of stress-strain relations in plasticity. It is further concluded that the initial shear modulus G_i is definitely not in agreement with the elastic shear modulus G_o as predicted by isotropic flow theories.

APPENDIX

1. General

The accuracy requirements and attendant difficulties peculiar to experimental investigations in plasticity, as opposed to the usual testing procedures in materials testing, have been emphasized recently by Drucker and Stokton[17]. Our Technical Report No. 1[4] outlined briefly how the experimental setup was being developed to include features necessary to meet these rather special requirements. This section records the details of the equipment as it is currently used, and describes developments and modifications that have been made since the issuance of Technical Report No. 1.

2. The Extensometer

Perhaps the most difficult feature of experimental studies in a state of combined stress is the measurement of the deformations of the specimens. This is particularly true when the state of stress is one of both tension and torsion.

In order to determine the average strains with sufficient resolution and precision over a reasonable gage length, a rather special extensometer is required. The main factors under consideration are that the extensometer should preferably have linear characteristics, the strain measurements should be independent, backlash and lag should be negligible, and finally it must lend itself to the coverage of a wide range of deformations, with comparable precision in both elastic as well as plastic regions. The fundamental features of such an instrument were presented in Technical Report No. 1. Referring to Fig. 4 of that report, which shows the extensometer in its original form, several rather basic alterations have been made.

The diametrical potentiometers (P_2) were found to have unsatisfactory resolution and were therefore removed. Several unsuccessful attempts were made to replace their function by a transducer that could measure circumference or diameter changes. These efforts were thwarted mainly by the difficulty of obtaining a reproducible calibration.

The angle of twist pick-up arm (A) was replaced by a double cantilever arrangement made up of thin flexure numbers as shown in Figs. 14 and 15. This modification considerably improved the response of the angle of twist measurement and eliminated a tendency to lag under reversal of torque.

The axial extension potentiometers (P_1) gave a great deal of trouble. Wear of contact areas on the sliders (C_1) and the very short range of motion (relative to the resistance-wire diameter) reduced the repeatibility and resolution to unacceptable values when both twist and extension were being recorded together. Although new contact materials and better resistance-wire material were tried, insufficient improvement was achieved. It finally proved necessary to replace these potentiometers by an extension unit utilizing SR-4 strain gages. This unit has proven through extensive tests to give the desired sensitivity and also the required independence of twist and extension. Figures 14 and 15 show the construction of this unit. Four phosphor bronze spring legs, having two SR-4 type A-7 gages each, are attached to the bottom disc (D). The other ends of these bent strips are fastened to a steel ring which has its top surface ground and polished. This ring serves as a base for three instrument bearings which are fixed to the underside of the top disc. The use of the four spring strip arms makes possible the averaging of any slight tilts that might occur between the two discs.*

As evidence of the repeatibility and linearity of the extensometer, typical calibration curves are included as Fig. 16.

3. Tension-Torsion Machine

A change in the tension-torsion machine was indicated due to a tendency of the upper load bar to stick in its sleeve bearing. Although an infrequent occurrence, it was quite bothersome. A ball-bearing arrangement substituted in part for the sleeve bearing considerably improved the situation and will possibly allow reversed twist tests to be performed.

4. Recording Oscillograph

In direct opposition to static elastic testing, experimental investigations in plasticity require that account be taken at all times of the rates of loading and straining. In this study, all variables are recorded continuously on a single oscillograph film. A facsimile of one such film for a variable-loading-path test is shown in Fig. 17. The convenience of having the data completely displayed as a continuous function of time is clearly seen in this typical record.

*It is, of course, not necessary to know the gage factor of the strain gages, since the unit may be calibrated.

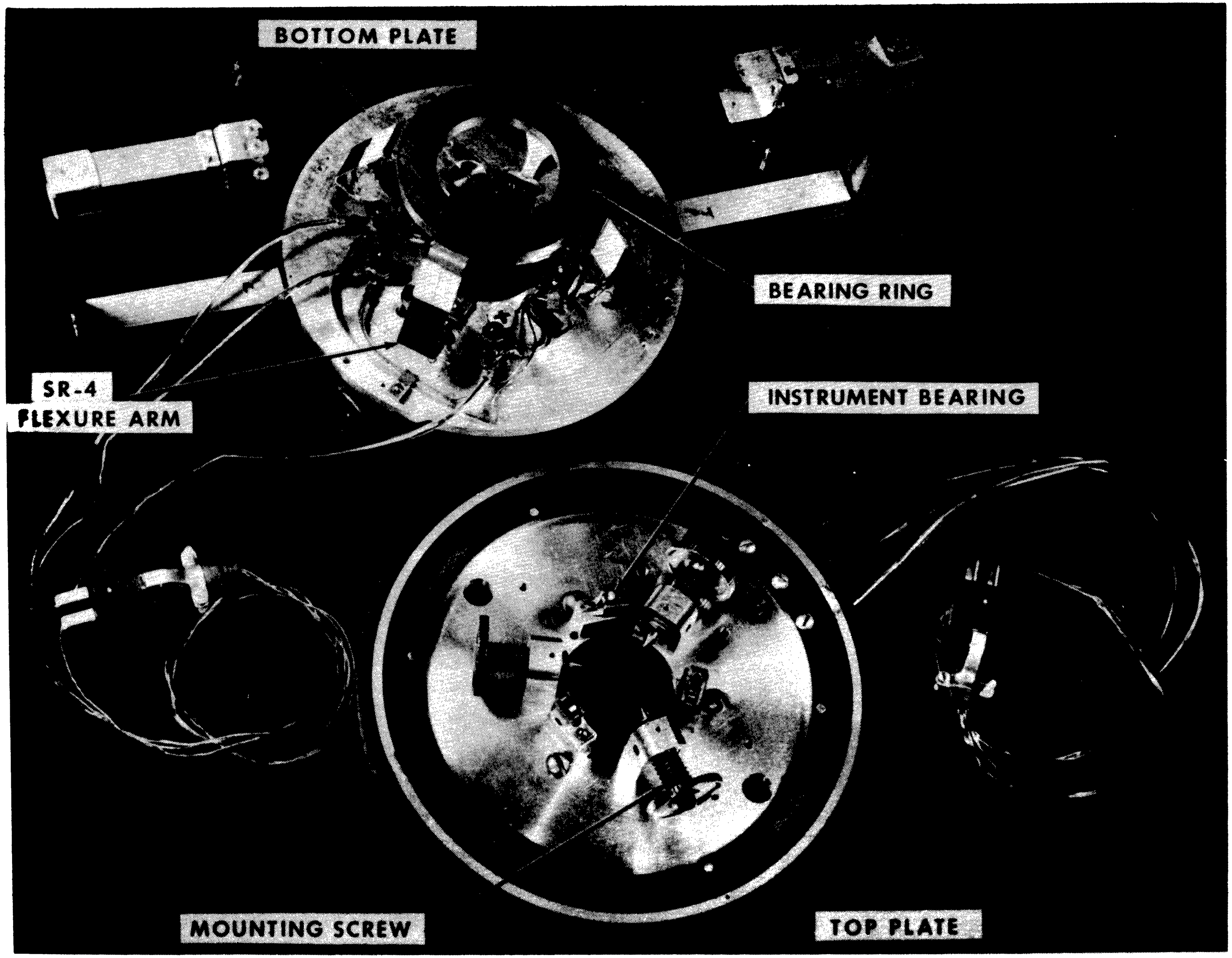
BOTTOM PLATE
BEARING RING
SR-4
FLEXURE ARM
INSTRUMENT BEARING
MOUNTING SCREW
TOP PLATE

Fig. 14

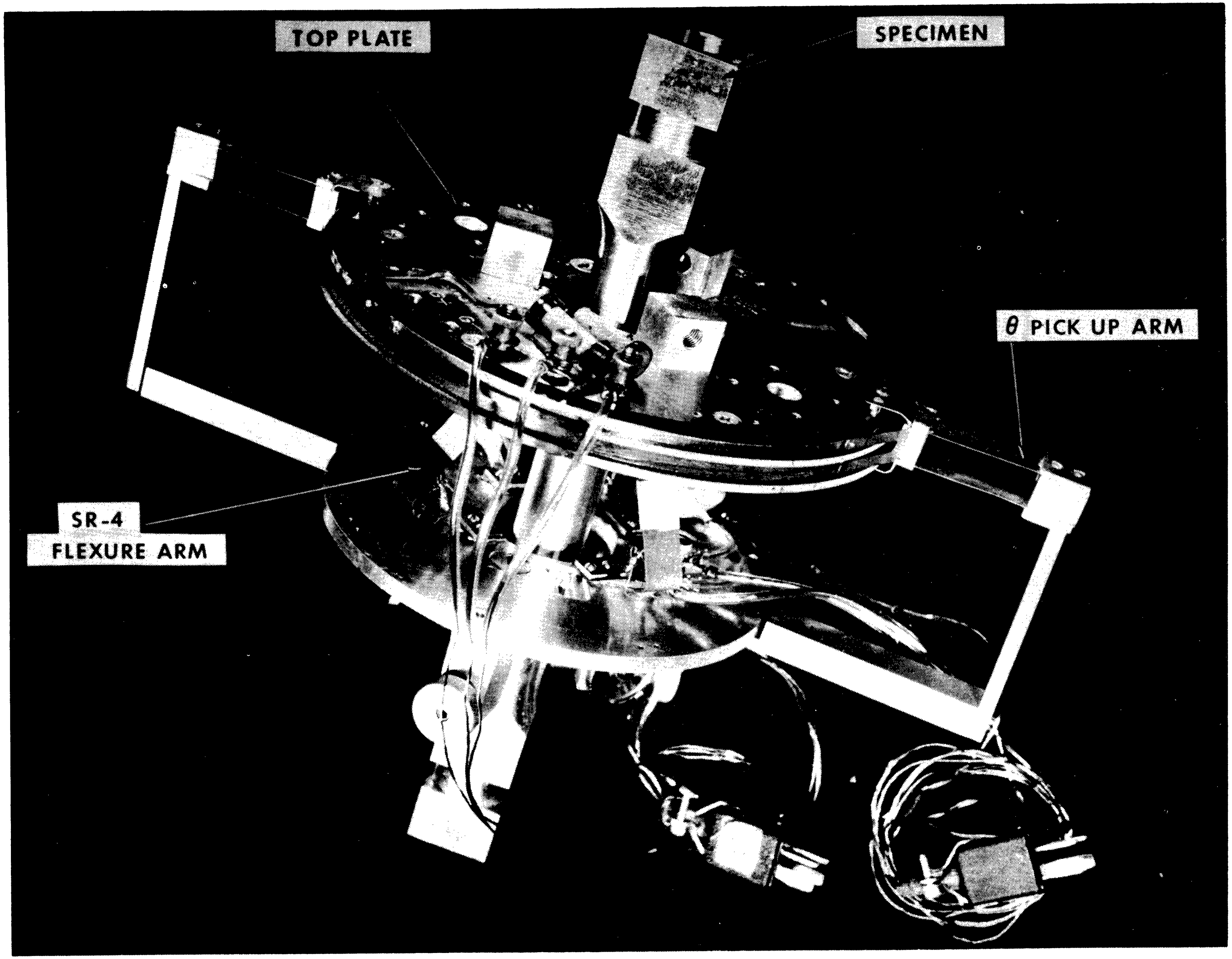

Fig. 15

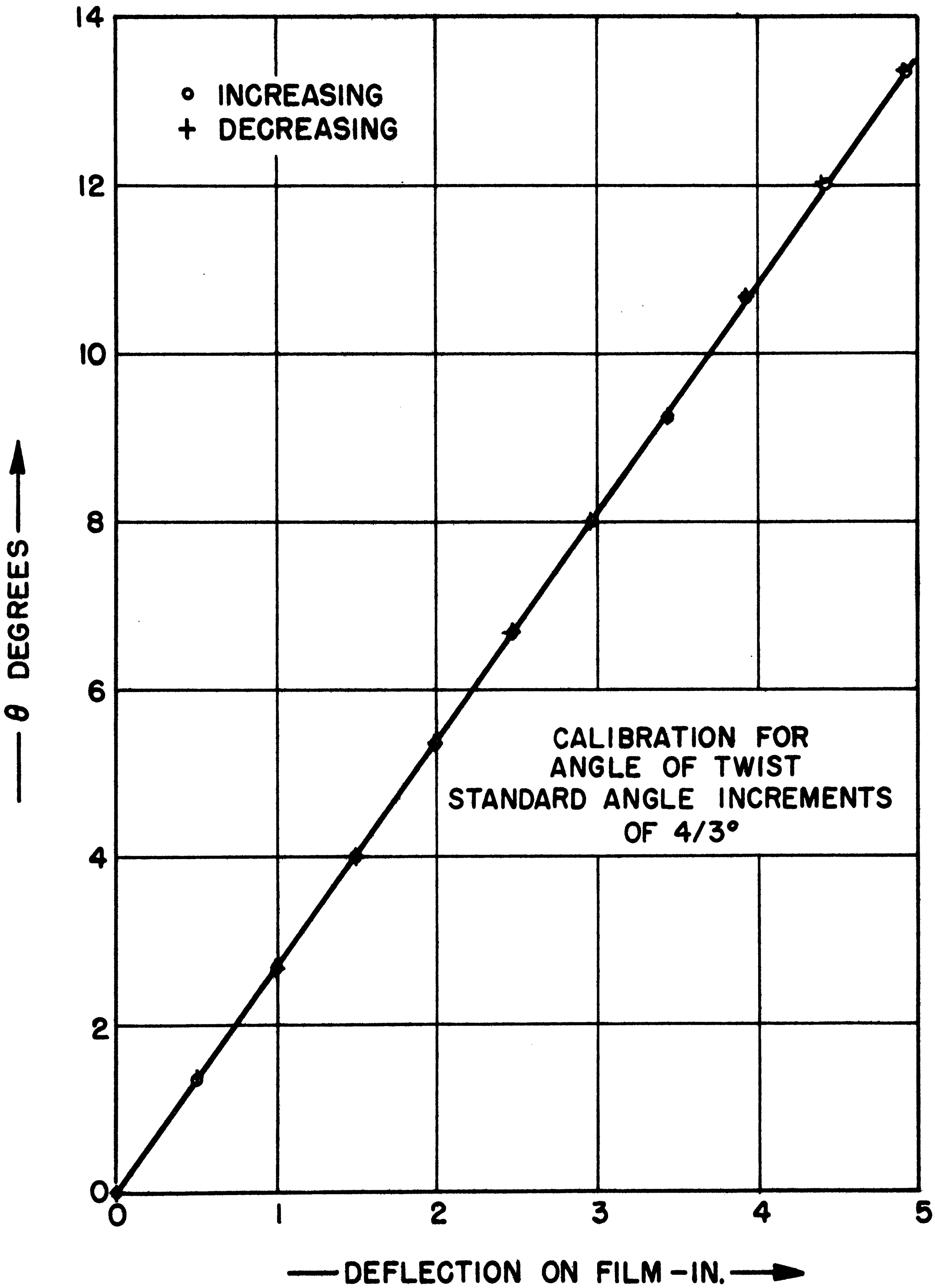

FIG. 16 CALIBRATION OF ANGLE OF TWIST

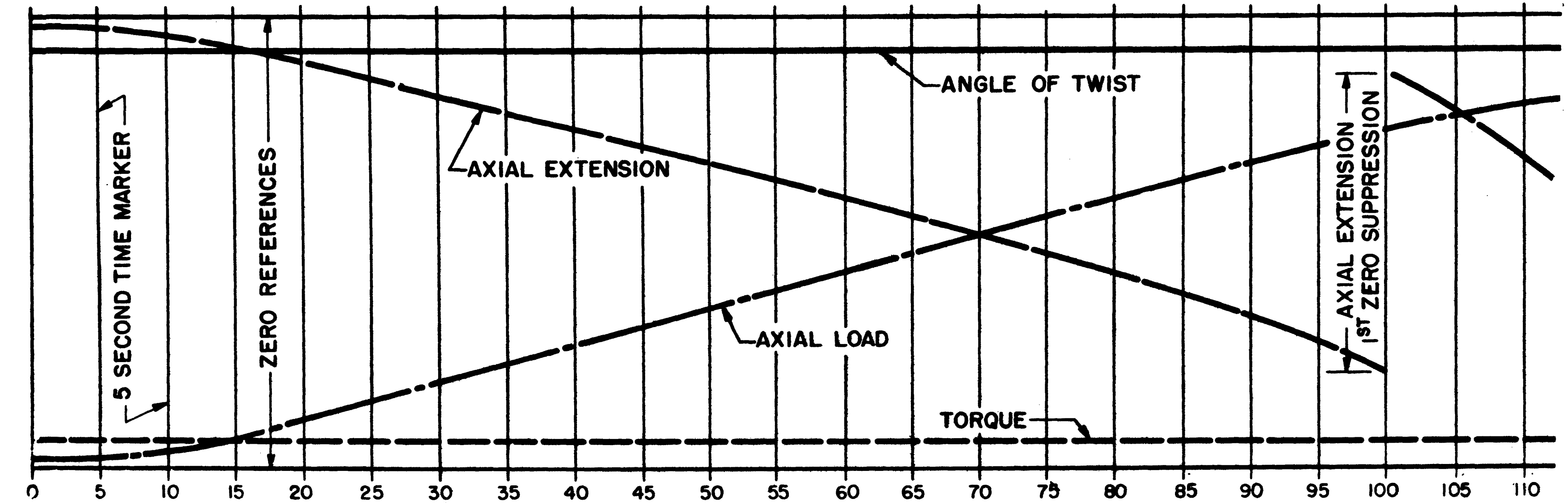

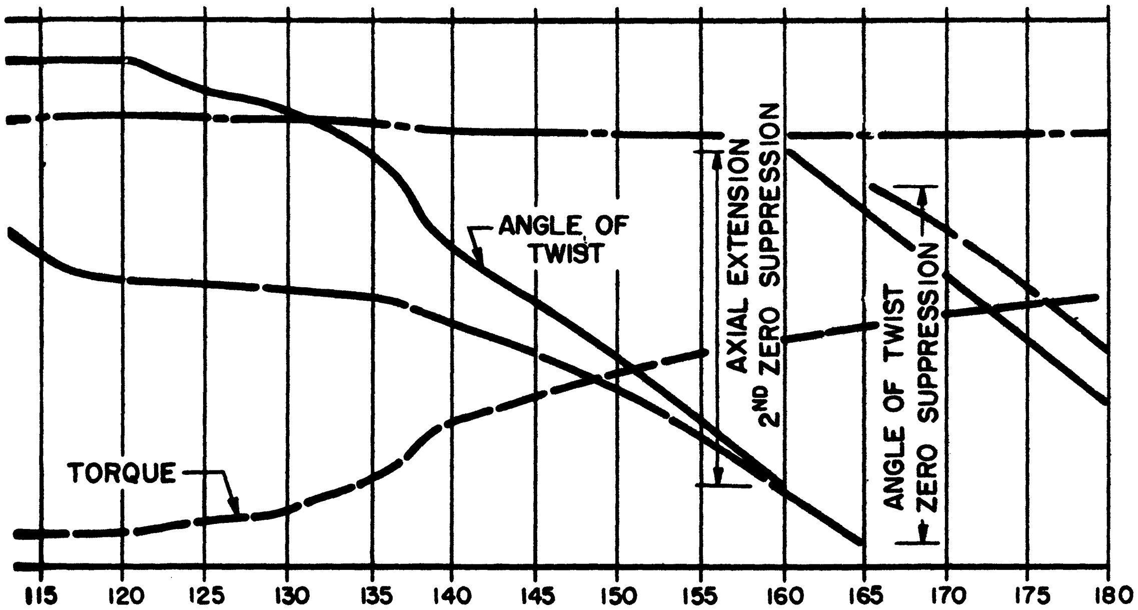

VARIABLE LOADING TEST

THIN WALLED TUBE SPECIMEN A-4 (#34)

LOADING PATH

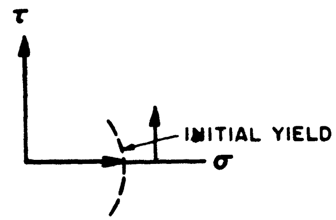

Fig. 17

The use of zero suppression is also indicated in Fig. 17. This method for allowing the record of any variable to be expanded over several widths of the 6-inch film makes possible a considerable increase in resolution.

For diagrams of the recording circuits, see Figs. 18 through 22.

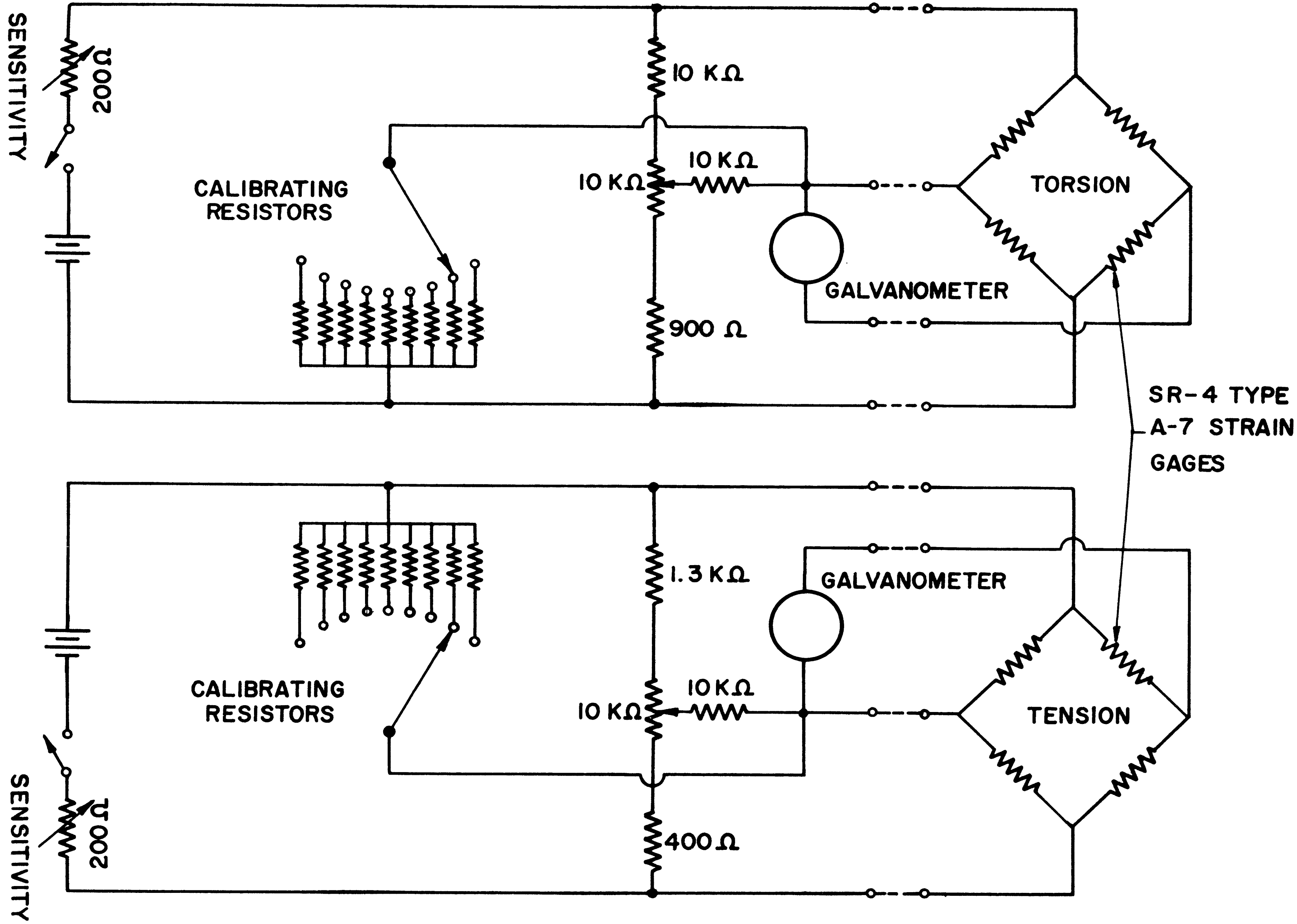

FIG. 18 LOAD DYNAMOMETER RECORDING CIRCUITS

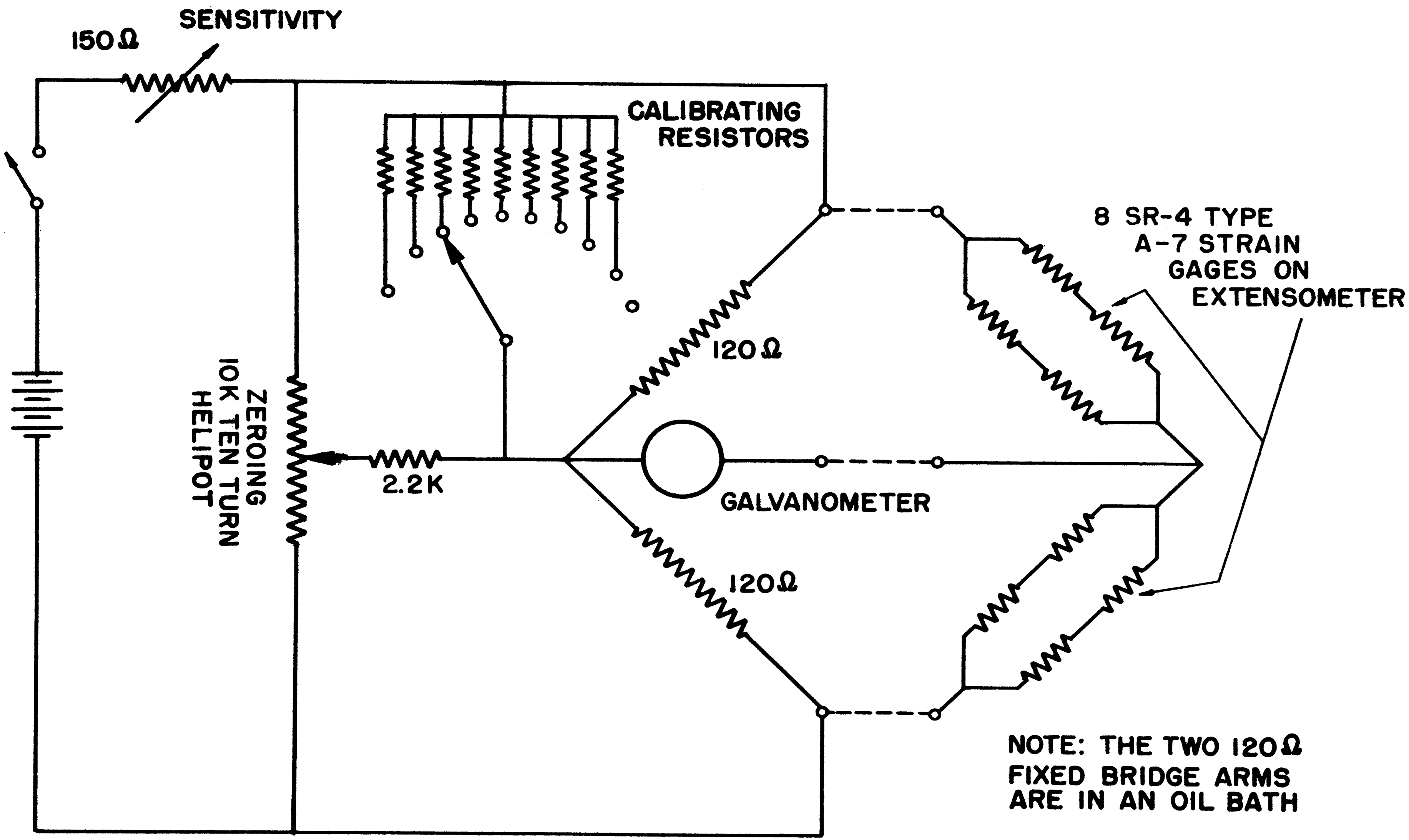

FIG. 19 CIRCUIT FOR RECORDING AXIAL EXTENSION

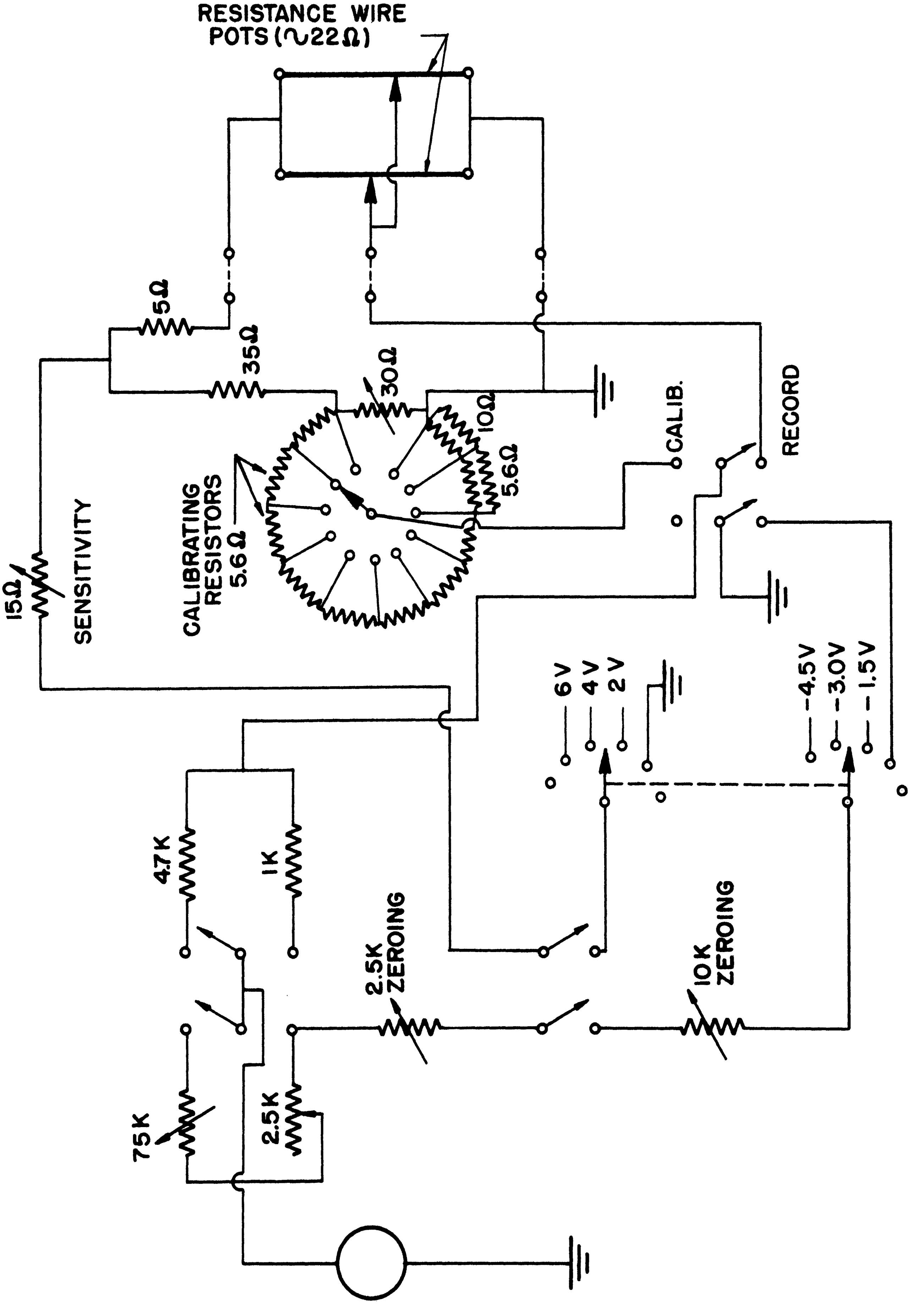

FIG.20 CIRCUIT FOR RECORDING ANGLE OF TWIST (POTENTIOMETER)

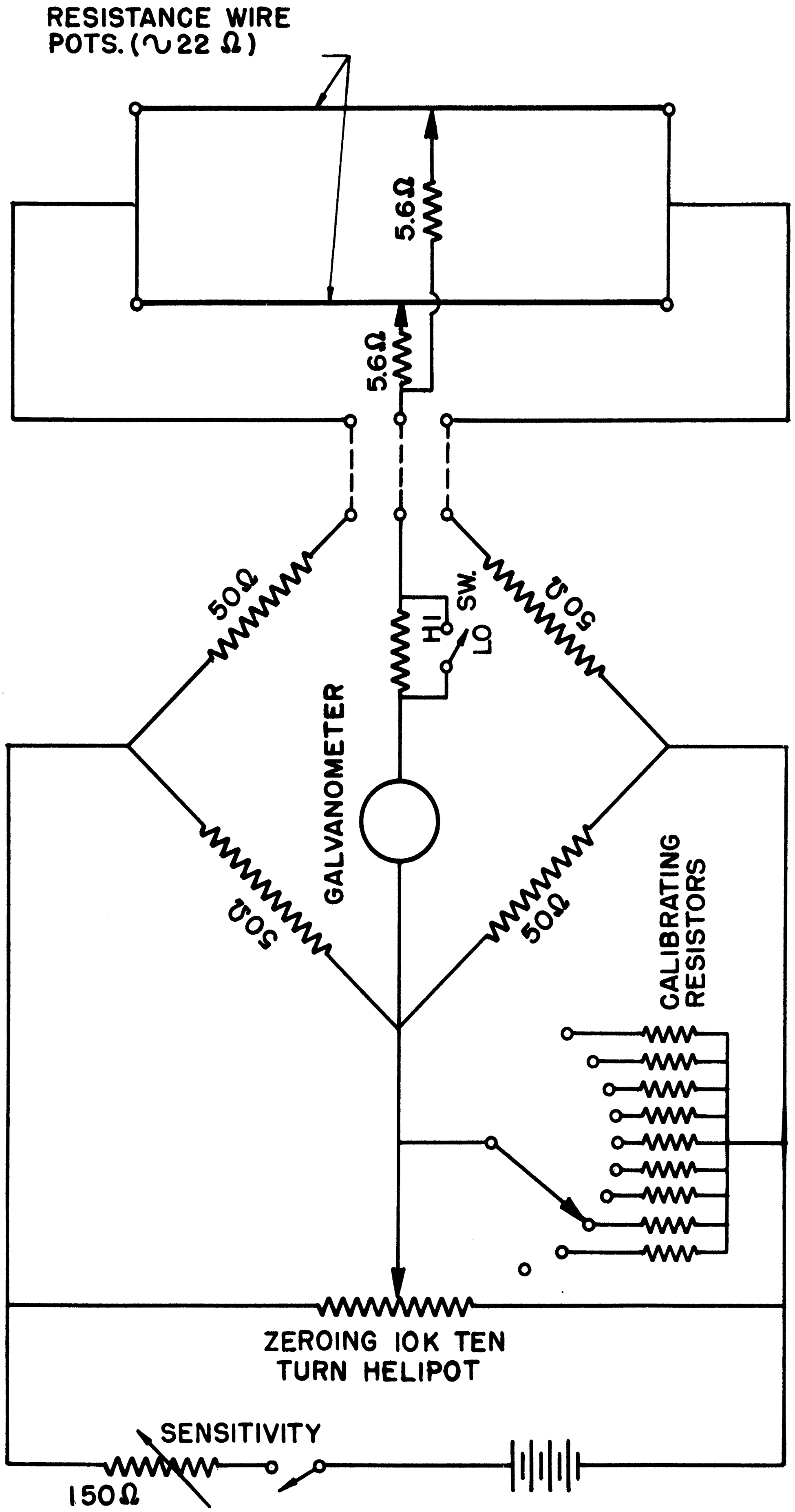

FIG. 21 CIRCUIT FOR RECORDING ANGLE OF TWIST. (BRIDGE)

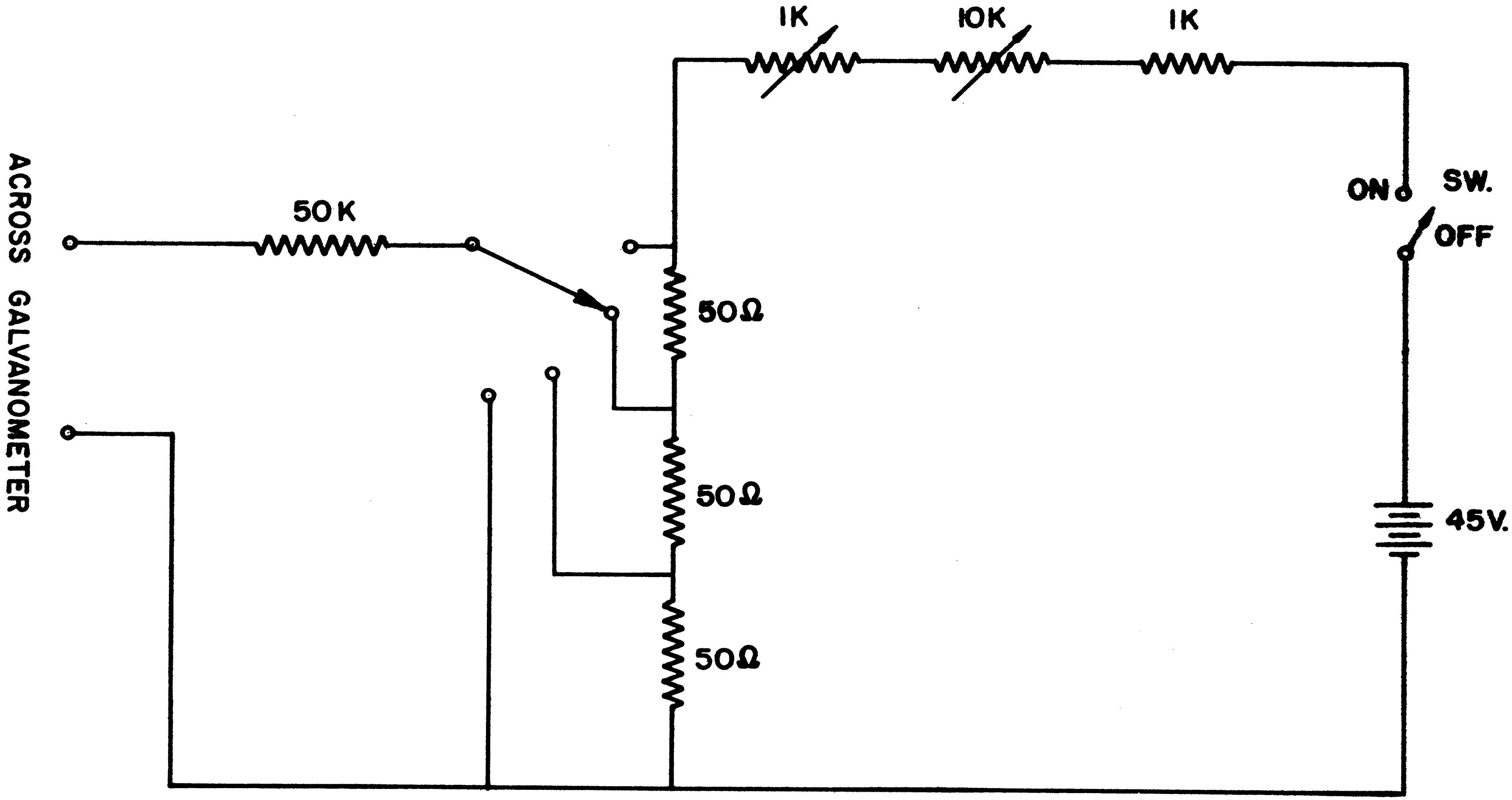

FIG. 22 ZERO SUPPRESSION CIRCUIT

REFERENCES

1. "Recent Developments in the Mathematical Theory of Plasticity", by W. Prager, J. Appl. Phys., 20, 235-241 (1949).

2. "The Stress-Strain Laws of the Mathematical Theory of Plasticity - A Survey of Recent Progress", by W. Prager, J. Appl. Mech., 15, 226-233 (1948).

3. "Some Extensions of Elementary Plasticity Theory", by F. Edelman and D. C. Drucker, J. Franklin Institute, 251, 581 (1951).

4. "Fundamental Experiments in Plasticity - Instrumentation and Preliminary Phase", by P. M. Naghdi and J. C. Rowley, O. O. R. Technical Report No. 1, University of Michigan, 1952.

5. "Stress-Strain Relations for Strain Hardening Materials - Discussion and Proposed Experiments", by D. C. Drucker, Proc. First Symp. Appl. Math., 1, 181-187 (1949).

6. "The Relation of Experiments to Mathematical Theories of Plasticity", by D. C. Drucker, J. Appl. Mech., 16, 349 (1949).

7. "The Significance of the Criterion for Additional Plastic Deformation of Metals", by D. C. Drucker, J. Colloid Science, 4, 299 (1949).

8. "On the Interpretation of Combined Torsion and Tension Tests of Thin-Wall Tubes", by W. Prager, NACA TN1501, 1948.

9. "A Mathematical Theory of Plasticity Based on the Concept of Slip", by S. B. Batdorf and B. Budiansky, NACA TN1871, April 1949.

10. "Stress-Strain Relations, Uniqueness and Variational Theorems for Elastic-Plastic Materials with a Singular Yield Surface", by W. T. Koiter, Quart. Appl. Math., 11, No. 3, 350-354 (1953).

11. "Strain Hardening Under Combined Stresses", by W. Prager, J. Appl. Phys., 16, 837-840 (1945).

12. "Preliminary Experiments for Testing Basic Assumptions of Plasticity Theory", by R. W. Peters, N. F. Dow, and S. B. Batdorf, Proc. Soc. Exp. Stress Analys., 7, No. 2, 127-140 (1949).

13. "Experimental Studies of Polyaxial Stress-Strain Laws of Plasticity", by B. Budiansky, N. F. Dow, R. W. Peters, and R. P. Shepherd, Proc. First U.S. National Congress Appl. Mech., 503-512 (1951).

14. "An Experimental Investigation of Plastic Stress-Strain Relations", by J. L. M. Morrison and W. M. Shepherd, Proc. Inst. Mech. Eng., 163, 1-9 (1950).

15. "On the Plastic Behavior of Thick Tubes under Combined Torsion and Internal Pressure", by B. Crossland, and R. Hill, J. Mech. and Phys. of Solids, 2, 27-38 (1953).

16. "A More Fundamental Approach to Plastic Stress-Strain Relations", by D. C. Drucker, Proc. First U.S. National Congress Appl. Mech., 487-491 (1951).

17. "Instrumentation and Fundamental Experiments in Plasticity", by D. C. Drucker and F. D. Stokton, to appear in Proc. Soc. Exp. Stress Analysis; also ONR Tech. Rept. No. 68, Brown University, 1952.

18. "Experimental Evidence of Non-Linearity in Plastic Stress-Strain Relations", by F. D. Stokton, ONR Tech. Rept. No. 88, Brown University, 1953.